

Electromagnetic Coupling with a Collinear Array on a Two-Layer Anisotropic Earth

GEOLOGICAL SURVEY PROFESSIONAL PAPER 1077



Electromagnetic Coupling with a Collinear Array on a Two-Layer Anisotropic Earth

By JEFFREY C. WYNN

CONTRIBUTIONS TO GEOPHYSICS

GEOLOGICAL SURVEY PROFESSIONAL PAPER 1077

A study of the effects of electromagnetic coupling in dipole-dipole and pole-dipole induced polarization field measurements, with evaluation of a coupling-removal technique



UNITED STATES DEPARTMENT OF THE INTERIOR

CECIL D. ANDRUS, *Secretary*

GEOLOGICAL SURVEY

H. William Menard, *Director*

Library of Congress Cataloging in Publication Data

Wynn, Jeffrey C.

Electromagnetic coupling with a collinear array on a two-layer anisotropic earth.

(Contributions to geophysics) (Geological Survey Professional Paper 1077)

Bibliography: p. 26

1. Induced polarization. 2. Anisotropy. I. Title. II. Series. III. Series:

United States Geological Survey Professional Paper 1077.

QC820.W96 538'.7 78-606005

For sale by the Superintendent of Documents, U.S. Government Printing Office
Washington, D.C. 20402
Stock Number 024-001-03169-8

CONTENTS

	Page		Page
Abstract	1	Theoretical development—Continued	
Introduction	1	Method of calculation	6
Acknowledgments	1	Model results	7
Theoretical development	1	Isotropic earth	7
Derivation of the general solution to EM coupling	1	Anisotropic earth	9
Horizontal component solution	3	The real world: rock response and coupling removal	10
Vertical component solution	3	Conclusions and computer results	13
		Selected references	26

ILLUSTRATIONS

		Page
FIGURE 1.	Diagram of a two-layer anisotropic-earth model	2
2.	Plots of behavior of the $\iint \mathbf{P}(r) dS ds$ and \hat{Q} functions	6
3.	Diagram of collinear electromagnetic arrays	6
4.	Diagram of an anisotropic earth with collinear dipole-dipole and pole-dipole arrays	6
5.	Plot of homogeneous-earth electromagnetic coupling	7
6.	Plots of pole-dipole and dipole-dipole coupling	7
7.	Diagram of complex resistivity relationships	8
8-17.	Plots of—	
8.	Coupling as a function of N-spacing	8
9.	Coupling as a function of D/A ratio	8
10.	Coupling from Willcox Playa, Ariz.	9
11.	Comparison of isotropic and anisotropic coupling	10
12.	Anisotropic coupling for changing N	10
13.	Anisotropic coupling for changing D/A	10
14.	Barren-rock spectrum in Cartesian coordinates	11
15.	Barren-rock spectrum in polar coordinates	11
16.	Altered-rock spectrum in Cartesian coordinates	12
17.	Altered-rock spectrum in polar coordinates	12

TABLES

		Page
TABLE 1.	IP parameters for a two-layer isotropic earth as a function of N-spacing	8
2.	IP parameters for a two-layer isotropic earth as a function of depth to the interface D/A	9
3.	Comparison of coupling removal results with laboratory results for three isotropic-earth coupling cases	13
4.	Comparison of coupling removal results with laboratory results for three anisotropic-earth coupling cases	13
5.	Electromagnetic coupling computer-program listings	13
6.	Examples of electromagnetic coupling for isotropic and anisotropic two-layer earth models	17

CONTRIBUTIONS TO GEOPHYSICS

ELECTROMAGNETIC COUPLING WITH A COLLINEAR ARRAY ON A TWO-LAYER ANISOTROPIC EARTH

By JEFFREY C. WYNN

ABSTRACT

The development of theoretical equations for calculating electromagnetic coupling commonly encountered in Induced Polarization (IP) field surveys is presented. For an isotropic earth with a resistive basement, the magnitude and phase angle of the electric field decrease as the induction parameter is increased. In the case of a conductive basement, the phase angle reaches a maximum negative shift, then increases with increasing induction parameter until it eventually becomes a phase lead. In this case the magnitude will also begin to increase at the higher frequencies.

For an anisotropic earth model, the magnitude may increase with increasing induction parameter in the low-frequency region, giving rise to a negative percent frequency effect (PFE). At higher frequencies, a "notch" may develop, but this latter feature will have little effect on field IP measurements.

A simple coupling-removal method is discussed and tested with model and laboratory data. In about half the cases this method worked reasonably well, its effectiveness diminishing as resistivities at the surface were reduced. For a conductive basement, the method fails consistently to remove the coupling contribution, due to the reversal of the phase shift. Because an anisotropic-earth model has phase shifts similar to isotropic models, the effectiveness of the removal method is not significantly reduced by the anisotropy.

Complete program listings in Fortran IV are included along with a representative suite of results plotted in the generalized Cartesian complex-plane format.

INTRODUCTION

Induced polarization (IP) surveys are carried out with the purpose of measuring the polarization parameters of the earth (Sumner, 1976). Unfortunately, in such surveys electromagnetic (EM) coupling produces the same *general* effects on the measurements as do the polarization parameters of the earth. The EM coupling consists of wire-to-wire inductive coupling and coupling through induction within the earth. Unless the EM coupling contribution is accurately removed, the IP measurements can be incorrectly interpreted as being caused by the polarization of the earth.

The effects of EM coupling can be quite variable. Lateral conductive inhomogeneities, whether geologic or cultural in origin, have the greatest effects on the IP measurement. By contrast, in many sedimentary environments lateral inhomogeneities are not usually present, and the EM coupling effects are more subtle. Because strong coupling effects are more obvious, this report investigates instead the more

subtle aspects of EM coupling arising from a layered, anisotropic earth. These subtle effects of EM coupling must be accounted for in order to correctly interpret high-precision IP survey data.

This paper describes the theoretical development of electromagnetic-coupling calculations for an anisotropic two-layer earth, for two commonly used collinear arrays, the dipole-dipole and the pole-dipole array. A computer program was written to perform the calculations and is included along with tabulated spectra for many different earth models. The data are presented in a generalized form of normalized real and imaginary components and are plotted in the Cartesian complex plane. A method is described for the extension of these results to percent frequency effect (PFE) and phase angle (ϕ) representations. Time-domain-IP chargeabilities can be obtained from the phase angle results, and the method for this is also shown.

ACKNOWLEDGMENTS

The laboratory and field electrical measurements were made while the author was employed by Zonge Engineering, Tucson, Ariz., using equipment designed by Dr. Kenneth L. Zonge. The theoretical calculations were made using the University of Arizona CDC 6400 and the U.S. Geological Survey DEC-10 computer.¹

THEORETICAL DEVELOPMENT

DERIVATION OF THE GENERAL SOLUTION TO EM COUPLING

The original calculations for EM coupling on a two-layer isotropic earth were made by Sunde (1967). Derivations for a multi-layer isotropic earth are also available in Anderson (1975). The general solution for EM coupling over a two-layer anisotropic earth can be obtained from boundary conditions and Maxwell's equations for layered media as follows.

¹Use of trade names in this report is for informative or descriptive purposes only and does not constitute endorsement by the U.S. Geological Survey.

Let us assume a two-layer geometry as in figure 1.

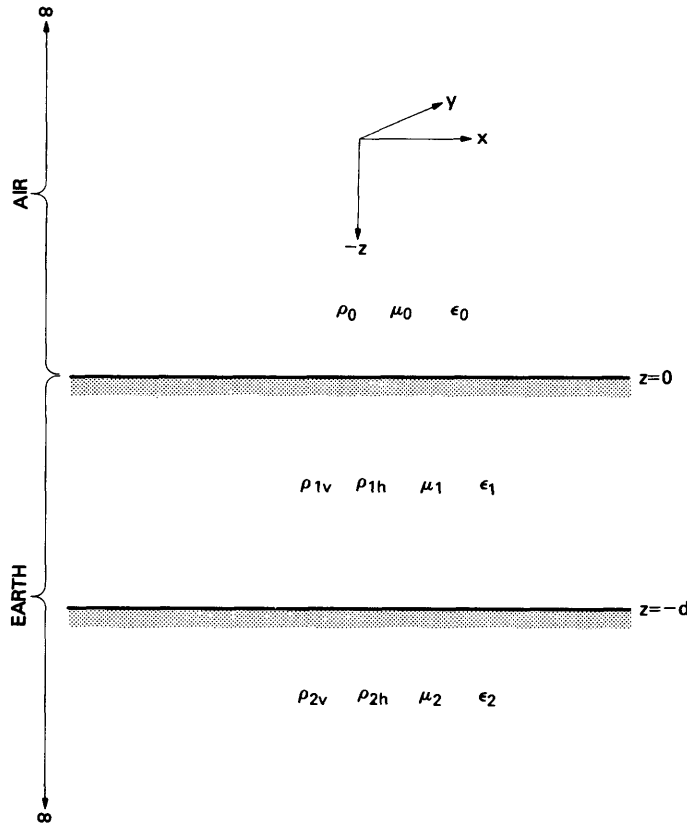


FIGURE 1.—Two-layer anisotropic-earth model. ρ_{jv} is the resistivity of the j th layer in the vertical direction; ρ_{jh} is the resistivity of the j th layer (0, 1, or 2 in this case) in the horizontal direction; x and y directions assumed to have the same resistivity; ϵ_j is magnetic permeability, and μ_j is dielectric permittivity of the j th layer. Z is the vertical direction.

Let $\gamma_j^2 = i\omega\mu_0\left(\frac{1}{\rho_j} + i\omega\epsilon_j\right)$, where $i = \sqrt{-1}$ for the j th layer.

In this equation, ϵ_j is the permittivity of the medium, μ_0 is the permeability of free space, ω is the angular frequency, ρ_j is the resistivity, the inverse of the resistivity is the conductivity σ_j , and γ_j is a propagation constant for electromagnetic waves in the medium.

Assuming the free space values $\epsilon_j = \epsilon_0$, $\mu_j = \mu_0$, and $\mu_0\epsilon_0 = 1.16 \times 10^{-17}$ in MKS units, then the quasistatic approximation (no displacement currents) can be made for the frequency range of interest and

$$\gamma_j^2 \approx i\omega\mu_0\sigma_j = \frac{i\omega\mu_0}{\rho_j}. \quad (1)$$

Writing the field equations in terms of the Hertz potential Π (Sunde, 1968, p. 102), we have:

$$H_x = \frac{\gamma_z^2}{i\omega\mu_0} \frac{\partial \Pi_z}{\partial y} \quad (2)$$

$$H_y = \frac{\gamma_x^2}{i\omega\mu_0} \left(\frac{\partial \Pi_x}{\partial z} - \frac{\partial \Pi_z}{\partial x} \right), \quad (3)$$

$$E_y = \frac{\partial}{\partial y} \left(\frac{\partial \Pi_x}{\partial x} - \frac{\partial \Pi_z}{\partial z} \right), \quad (4)$$

$$E_x = -\gamma_x^2 \Pi_x + \frac{\partial}{\partial x} \left(\frac{\partial \Pi_x}{\partial x} + \frac{\partial \Pi_z}{\partial z} \right), \quad (5)$$

$$H_z = 0, \quad (6)$$

and

$$E_z = -\gamma_z^2 \Pi_z + \frac{\partial}{\partial z} \left(\frac{\partial \Pi_x}{\partial x} + \frac{\partial \Pi_z}{\partial z} \right). \quad (7)$$

where we have set $\Pi_y = 0$ for the x - z excitation case considered here and H and E refer to the magnetic and electric field components, respectively.

Eight equations may be developed from the condition that requires the tangential components to be continuous across the boundaries between the different media. Let the horizontal components be labeled h ; then at the earth-air interface ($z=0$) and at a layer interface ($z=-d$) we obtain:

Earth-air interface
 $z=0$

Layer interface
 $z=-d$

$$\gamma_0^2 \Pi_{0z} = \gamma_{1z}^2 \Pi_{1z}, \quad (8a) \quad \gamma_{1z}^2 \Pi_{1z} = \gamma_{2z}^2 \Pi_{2z}, \quad (8b)$$

$$\gamma_0^2 \frac{\partial \Pi_{0h}}{\partial z} = \gamma_{1h}^2 \frac{\partial \Pi_{1h}}{\partial z}, \quad (9a) \quad \gamma_{1h}^2 \frac{\partial \Pi_{1h}}{\partial z} = \gamma_{2h}^2 \frac{\partial \Pi_{2h}}{\partial z}, \quad (9b)$$

$$\frac{\partial \Pi_{0h}}{\partial h} + \frac{\partial \Pi_{0z}}{\partial z} = \frac{\partial \Pi_{1h}}{\partial h} + \frac{\partial \Pi_{1z}}{\partial z} = \frac{\partial \Pi_{2h}}{\partial h} + \frac{\partial \Pi_{2z}}{\partial z}, \quad (10a) \quad (10b)$$

$$\gamma_0^2 \Pi_{0h} = \gamma_{1h}^2 \Pi_{1h}, \quad (11a) \quad \gamma_{1h}^2 \Pi_{1h} = \gamma_{2h}^2 \Pi_{2h}. \quad (11b)$$

(Equations 9a, b were simplified by equations 8a, b; equations 11a, b were simplified using equations 10a, b.)

Let us assume a general solution for the Hertz potential (Sunde, 1968) of

$$\pi_j = \cos \phi \int_0^\infty [f(\lambda) e^{U_j z} + g(\lambda) e^{-U_j z}] J_n(r\lambda) d\lambda,$$

where r is the total distance from the point electrode, ϕ is an azimuthal angle, $\cos \phi = x/r$, λ is an integration variable, and J_n is an n th order Bessel function of the first kind (real

argument). The function U_j is a propagation constant, and

$$U_{jh} = (\lambda^2 + \gamma_{jh}^2)^{1/2}$$

for the horizontal component, and

$$U_{jv} = (\lambda^2 + \gamma_{jv}^2)^{1/2}$$

for the vertical component. For horizontal components, $\phi = 0$.

HORIZONTAL COMPONENT SOLUTION

$$\pi_{oh} = \int_0^\infty [f_0 e^{\lambda z} + g_0 e^{-\lambda z}] J_0(r\lambda) d\lambda$$

at $z=0$,

$$\pi_{lh} = \int_0^\infty [f_1 e^{u_{lh} z} + g_1 e^{-u_{lh} z}] J_0(r\lambda) d\lambda$$

where $-d \leq z \leq 0$, and

$$\pi_{2h} = \int_0^\infty f_3 e^{u_{2h} z} J_0(r\lambda) d\lambda$$

where $z \leq -d$. Note that f_j and g_j are functions used to satisfy the boundary conditions for the j th layer. Then, using the four boundary conditions 9a, 9b, 11a, 11b, we obtain the following equations at $z=0$ and $z=-d$:

$$\gamma_0^2 \lambda (f_0 - g_0) = \gamma_{1h}^2 u_{1h} (f_1 - g_1), \quad (12)$$

$$\gamma_0^2 (f_0 + g_0) = \gamma_{1h}^2 (f_1 + g_1), \quad (13)$$

$$\gamma_{1h}^2 u_{1h} (f_1 e^{-u_{1h} d} - g_1 e^{u_{1h} d}) = \gamma_{2h}^2 u_{2h} f_2 e^{-u_{2h} d}, \quad (14)$$

and

$$\gamma_{1h}^2 (f_1 e^{-u_{1h} d} + g_1 e^{u_{1h} d}) = \gamma_{2h}^2 f_2 e^{-u_{2h} d}. \quad (15)$$

At this stage we will simplify the subscript notation by: $1h \rightarrow 1$, $1z \rightarrow 3$, $2z \rightarrow 4$, and $2h \rightarrow 2$.

Equations 12 to 15 can be reduced by algebra to:

$$f_1 = f_0 \frac{\gamma_0^2}{\gamma_1^2} \frac{2\lambda(u_1 + u_2)}{\Delta}, \quad (16)$$

and

$$g_1 = f_0 \frac{\gamma_0^2}{\gamma_1^2} \frac{2\lambda(u_1 - u_2) e^{-2u_1 d}}{\Delta}, \quad (17)$$

where

$$\Delta = (u_2 + u_1)(u_1 + \lambda) + (u_2 - u_1)(u_1 - \lambda) e^{-2u_1 d}. \quad (18)$$

If we make a temporary assumption of a homogeneous whole space, $\gamma_0 = \gamma_1 = \gamma_2 = \gamma_3 = \gamma_4$, by setting $g_1 = 0$ and $f_0 = f_1$ and solving the resulting equations, we obtain

$$f_0 = IdS \frac{i\omega\mu_0}{4\pi\gamma_0^2\lambda}.$$

For wires on the surface of the earth, this gives:

$$f = IdS \frac{i\mu_0\omega}{4\pi} \frac{2\lambda(u_1 + u_2)}{\gamma_1^2 \Delta}, \quad (19)$$

and

$$g_1 = IdS \frac{i\mu_0\omega}{4\pi} \frac{2\lambda(u_1 - u_2)}{\gamma_1^2 \Delta} e^{-2u_1 d}, \quad (20)$$

where dS is the infinitesimal segment of the source dipole carrying a current I .

VERTICAL COMPONENT SOLUTION

For the vertical components,

$$\pi_{oz} = \cos \phi \int_0^\infty p_0 e^{-\lambda z} J_1(r\lambda) d\lambda$$

at $z=0$,

$$\pi_{1z} = \cos \phi \int_0^\infty [p_1 e^{u_3 z} + q_1 e^{-u_3 z}] J_1(r\lambda) d\lambda$$

where $-d \leq z \leq 0$,

$$\pi_{2z} = \cos \phi \int_0^\infty p_2 e^{u_4 z} J_1(r\lambda) d\lambda$$

where $z \leq -d$, and the p 's and q 's are functions used to satisfy the boundary conditions exactly like the f 's and g 's.

Using boundary conditions 8a, 8b, 10a, 10b, we can obtain

$$\gamma_3^2 (p_1 + q_1) = \gamma_0^2 p_0, \quad (21)$$

$$\gamma_3^2 (p_1 e^{-u_3 d} + q_1 e^{u_3 d}) = \gamma_4^2 p_2 e^{-u_4 d}, \quad (22)$$

$$\gamma_0^2 u_3 (p_1 - q_1) = (\gamma_0^2 - \gamma_3^2) \lambda (f_1 + g_1) - \gamma_0^2 \lambda p_0, \quad (23)$$

and

$$u_3 \gamma_2^2 (p_1 e^{-u_3 d} - q_1 e^{u_3 d}) = \gamma_2^2 p_2 u_4 e^{-u_4 d} + \lambda (\gamma_2^2 - \gamma_1^2) (f_1 e^{-u_1 d} + q_1 e^{u_1 d}). \quad (24)$$

We can then obtain the p's and q's by using algebra:

$$p_1 = \frac{\lambda(\gamma_0^2 - \gamma_1^2)(f_1 + g_1)\Delta_1'}{\Delta_0''\Delta_1''e^{-2u_3d} + \Delta_0'\Delta_1'} + \frac{\lambda(\gamma_2^2 - \gamma_1^2)[f_1e^{(-u_1+u_3)d} + g_1e^{(u_1-u_3)d}]\Delta_0''}{\Delta_0''\Delta_1''e^{-2u_3d} + \Delta_0'\Delta_1'}, \quad (25)$$

and

$$q_1 = \frac{\lambda(\gamma_1^2 - \gamma_2^2)[f_1e^{(-u_1+u_3)d} + g_1e^{(u_1-u_3)d}]\Delta_0'}{\Delta_0''\Delta_1''e^{-2u_3d} + \Delta_0'\Delta_1'} + \frac{\lambda(\gamma_0^2 - \gamma_1^2)(f_1 + g_1)\Delta_1''e^{-2u_3d}}{\Delta_0''\Delta_1''e^{-2u_3d} + \Delta_0'\Delta_1'}, \quad (26)$$

where:

$$\Delta_0'' = \lambda\gamma_3^2 - u_3\gamma_0^2,$$

$$\Delta_1'' = \gamma_2^2\left(u_3 - \frac{u_4\gamma_3^2}{\gamma_4^2}\right),$$

$$\Delta_0' = u_3\gamma_0^2 + \lambda\gamma_3^2, \text{ and}$$

$$\Delta_1' = \gamma_2^2\left(u_3 + \frac{u_4\gamma_3^2}{\gamma_4^2}\right). \quad (27)$$

Now utilizing equations 4 and 5 we can obtain:

$$E_x = -\gamma_1^2 \int_0^\infty (f_1 + g_1) J_0(r\lambda) d\lambda + \frac{\partial}{\partial x} \cos\phi \int_0^\infty [-\lambda(f_1 + g_1) + u_3(p_1 - q_1)] J_0(r\lambda) d\lambda$$

and

$$E_y = \frac{\partial}{\partial y} \cos\phi \int_0^\infty [-\lambda(f_1 + g_1) + u_3(p_1 - q_1)] J_1(r\lambda) d\lambda,$$

which reduces to

$$E_x = \text{IdS}\left[-\mathbf{P}(r) + \frac{\partial^2 \mathbf{Q}(r)}{\partial x^2}\right] \quad (28)$$

and

$$E_y = \text{IdS}\left[\frac{\partial^2 \mathbf{Q}(r)}{\partial x \partial y}\right], \quad (29)$$

where

$$\text{IdS}\mathbf{P}(r) = \lambda_1^2 \int_0^\infty (f_1 + g_1) J_0(r\lambda) d\lambda \text{ and} \quad (30)$$

$$\text{IdS}\mathbf{Q}(r) = \int_0^\infty [f_1 + g_1 - \frac{u_3}{\lambda}(p_1 - q_1)] J_0(r\lambda) d\lambda. \quad (31)$$

These results are the anisotropic analog of Riordan and Sunde's (1933) derivation. They can be generalized using a transformation similar to that suggested by Wait (1966): Let $G = \delta\lambda$, $B = r/\delta$; and $D = d/\delta$, where

$$\delta = \left(\frac{2\rho_1}{\mu_0\omega}\right)^{1/2}.$$

In addition let

$$\text{XKH} = \frac{\rho_1}{\rho_2}, \text{ AN1} = \frac{\rho_1}{\rho_3}, \text{ and AN2} = \frac{\rho_1}{\rho_4}.$$

These parameters XKH, AN1 and AN2 are used in the computer program in table 5. Then:

$$\gamma_1^2 = \frac{2i}{\delta^2}, \gamma_4^2 = \frac{2i}{\delta^2} \text{AN2} \dots$$

$$\text{and } U = \delta U_1 = (G^2 + 2i)^{1/2},$$

$$V = \delta U_2 = (G^2 + 2i \cdot \text{XKH})^{1/2},$$

$$W = \delta U_3 = (G^2 + 2i \cdot \text{AN1})^{1/2},$$

$$Y = \delta U_4 = (G^2 + 2i \cdot \text{AN2})^{1/2},$$

$$\text{and } \Delta_0'' = \Delta_0' = 2iG \cdot \frac{\text{AN1}}{\delta^3},$$

$$\Delta_1' = \frac{2i \cdot \text{XKH}}{\delta^3} \left[W + Y \frac{\text{AN1}}{\text{AN2}} \right],$$

$$\Delta_1'' = \frac{2i \cdot \text{XKH}}{\delta^3} \left[W - Y \frac{\text{AN1}}{\text{AN2}} \right],$$

$$\theta = A \sqrt{\frac{\omega\mu_0}{\rho_1}},$$

where A is the receiver dipole length, and θ is the generalized induction parameter.

The results of the transformation are:

$$f_1 = \frac{\omega\mu_0 G \delta^2}{4\pi\Delta'} [U+V],$$

$$g_1 = \frac{\omega\mu_0 G \delta^2}{4\pi\Delta'} [U-V] e^{-2UD},$$

$$p_1 = \frac{2iG}{\delta^3} \frac{-(f_1+g_1)\Delta'_1 + (XKH-1)(f_1 e^{-(U+W)D} + g_1 e^{(U-W)D})\Delta''_0}{\Delta''_0 \Delta'_1 e^{-2WD} + \Delta'_0 \Delta'_1},$$

$$q_1 = \frac{2iG}{\delta^3} \frac{(1-XKH)(f_1 e^{-(U+W)D} + g_1 e^{(U-W)D})\Delta'_0 - (f_1+g_1)\Delta''_1 e^{-2WD}}{\Delta''_0 \Delta'_1 e^{-2WD} + \Delta'_0 \Delta'_1}, \text{ and}$$

$$\Delta' = (g+U)(U+V) + (g-U)(U-V)e^{-2UD}.$$

Lastly:

$$\mathbf{P}(r) = \frac{2i}{\delta^3} \int_0^\infty [f_1 + g_1] \mathbf{J}_0(Bg) dg \quad (32)$$

and

$$\mathbf{Q}(r) = \int_0^\infty \frac{[f_1 + g_1 - \frac{W}{G}(p_1 - q_1)] \mathbf{J}_0(Bg) dg}{\delta}. \quad (33)$$

This transformation permits a broader application of the results of the numerical integration. Therefore, for instance, behavior of $\mathbf{P}(r)$ and $\mathbf{Q}(r)$ depends only on a resistivity ratio instead of on two separate values of resistivities. Results are always tabulated in terms of a generalized induction parameter,

$$\theta = A \sqrt{\frac{\omega\mu}{\rho_1}},$$

so that with a given spectrum in the complex plane, results can be calculated for different values of the receiver dipole spacing, A , or surface resistivity, ρ_1 , or angular frequency, ω .

At this point we should comment on the behavior of the two functions \mathbf{P} and \mathbf{Q} . For a homogeneous earth, \mathbf{Q} is constant and real, is frequency-independent, and contributes the resistive component to the mutual coupling. Over a two-layer earth, the \mathbf{Q} function becomes dependent upon frequency and varies with the distances between grounding points, the interface-depth-to-dipole-length, D/A , and the resistivity contrast, ρ_1/ρ_2 , between the two media. When evaluated over the two dipoles, \mathbf{Q} yields only four terms dependent on distances between grounding points and is a simple scalar function.

The \mathbf{P} function, on the other hand, is dependent upon the orientation of the dipoles. The mutual impedance includes a cosine term when integrated over the two dipoles:

$$\mathbf{P} = \int_A^B \int_D^E \mathbf{P}(r) \cos\phi dS ds. \quad (34)$$

Here, ϕ is the angle between the two elements dS and ds , referring to separate line segments. For these reasons, the \mathbf{P} function can be called the inductive term, and the \mathbf{Q} function can be called the grounding term. The behavior of these functions is illustrated in figure 2. In this figure $\hat{\mathbf{Q}}$ is a sum of \mathbf{Q} terms each of which is calculated for a separate electrode-electrode distance. This will be examined in more detail later.

For two infinitely long wires, \mathbf{Q} behaves asymptotically as $1/r$, and goes to zero as r becomes infinite. It goes to zero whether the wires are parallel or perpendicular. For two perpendicular wires over a one-dimensional earth, the \mathbf{P} term is zero. Therefore for two infinite, perpendicular wires, irrespective of the layering beneath them, the total electromagnetic coupling becomes zero. For a three-electrode array, the \mathbf{Q} function reduces from four to two terms, and for a two-electrode array with two infinite electrodes, \mathbf{Q} is further reduced to a single term. Diagrams of these arrays are shown in figure 3. Because \mathbf{P} must be evaluated by integrating over both dipoles by incremental lengths, the following results will not include coupling for three- or two-electrode arrays. The necessary computer time for the \mathbf{P} term increases as the product of the incremental lengths over which the function must be integrated, and the author felt that the computer time necessary for accurate evaluation was not justified in light of the infrequent use of these geometries.

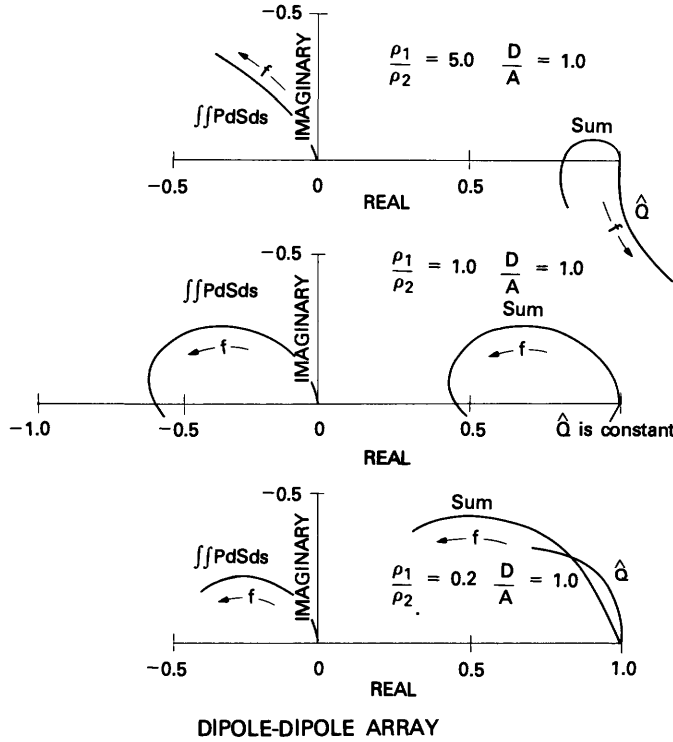


FIGURE 2—Behavior of $\iint P(r) dS ds$, the inductive component of EM coupling; \hat{Q} , the conductive component of EM coupling; and their sum as a function of resistivity contrast for an isotropic earth. The functions are plotted in the Cartesian complex plane, f shows the direction of increasing frequency, and all values are normalized by the real dc (direct-current) component.

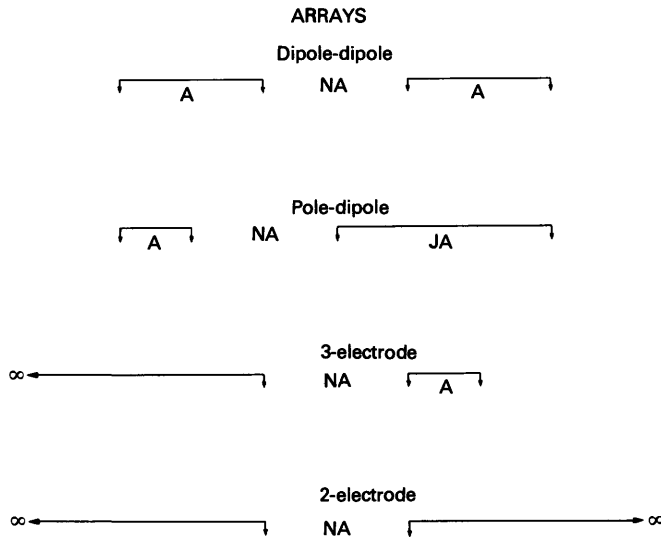


FIGURE 3.—Collinear arrays commonly used in the field, presented in order of frequency of use. N and J are multipliers of dipole length, A .

A note should also be added concerning anisotropy. Anisotropic P and Q kernel functions (mathematical sense) are included in the program listing in table 5 of this report

and are called ANISOP(x) and ANISOQ(x). In general these functions require twice the computer time for anisotropic conditions as that required for isotropic P and Q kernel functions. The isotropic function subroutines used for the majority of the calculations are called PDP(x) and PDQ(x) and are also included in the computer program listings in table 5.

METHOD OF CALCULATION

In general, the integrals of equations 32 and 33 cannot be evaluated analytically, so numerical integration was employed using the following procedure. The general form of the integrals can be represented as:

$$\int_0^{\infty} F(\lambda, r) J_n(\lambda r) d\lambda,$$

where $J_n(\lambda r)$ is the real component and $F(\lambda, r)$ is in general the complex component. The integral was evaluated as a sum of integrals between zeros of the Bessel function J_n . The first term, from zero (0.0) to the first zero of the Bessel function, was calculated using an adaptive Simpson's rule (Anderson, 1975), which divides the interval into smaller and smaller pieces until the iterated calculations repeat to within a user-specified precision. The next four terms were integrated using a sixteen-point Gaussian quadrature method, the ensuing series of terms were then integrated using an eight-point Gaussian quadrature method, and an Euler transformation was used to force convergence of the series. Precision was generally obtained to four decimal places by the sixteenth zero of the Bessel function.

In order to calculate the coupling for collinear dipole-dipole and pole-dipole arrays, the configuration shown in figure 4 was used.

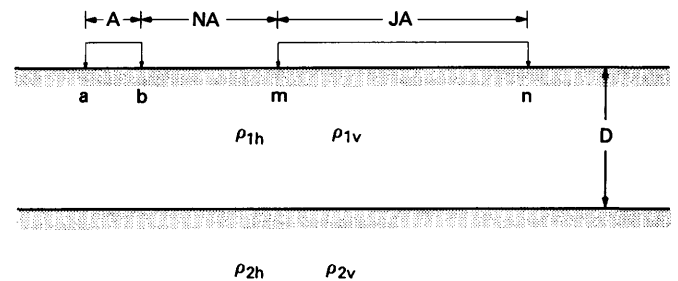


FIGURE 4.—Model cross section of an anisotropic earth showing collinear dipole-dipole and pole-dipole geometries. N and J are multipliers of dipole length A ; a , b , m , and n are electrodes.

In this figure and in subsequent equations, J is a multiplier indicating the length of the transmitter dipole with respect to the length of the receiver dipole.

A collinear dipole-dipole array is a specific subset of the collinear pole-dipole array, with $J=1$. To obtain the mutual impedance,

$$dZ_{Ss} = dSds \left[\mathbf{P}(r) \cos \phi + \frac{\partial^2 \mathbf{Q}(r)}{\partial S \partial s} \right], \quad (35)$$

one must evaluate the following:

$$Z_{Ss} = \sum_{m=1}^M \sum_{l=1}^{JM} \mathbf{P}(r) \frac{A^2}{M^2} + \hat{\mathbf{Q}}(a-b, m-n), \quad (36)$$

and

$$\frac{Z_{Ss}}{Z_0} = \frac{2\pi A^2}{\rho_1 M^2} \sum_{m=1}^M \sum_{l=1}^{JM} \mathbf{P}(r) + \frac{2\pi A}{\rho_1} \hat{\mathbf{Q}}(r), \quad (37)$$

where $\hat{\mathbf{Q}}(r) = \mathbf{Q}(am) - \mathbf{Q}(an) - \mathbf{Q}(bm) + \mathbf{Q}(bn)$.

In these equations, Z_{Ss} is the mutual impedance between the two dipoles S and s , and Z_0 is the dc (direct-current) coupling (resistive only) normalization factor. M is the number of segments that the dipoles are broken up into for purposes of integration.

It has been observed that four-place precision can be obtained for the pole-dipole configuration for any length of J greater than 7 to 10. In effect then, the pole-dipole array can be calculated with about 10 times the CPU (Central Processing Unit) time required for a dipole-dipole calculation.

An estimate of the convergence of Z_{Ss}/Z_0 against the number, M , of intervals that the dipoles should be broken up into can be obtained by comparing the homogeneous earth (with $\hat{\mathbf{Q}}$ constant) dipole-dipole results with the results using Millett's (1967) equations for a summation parameter $K=15$ (fig. 5).

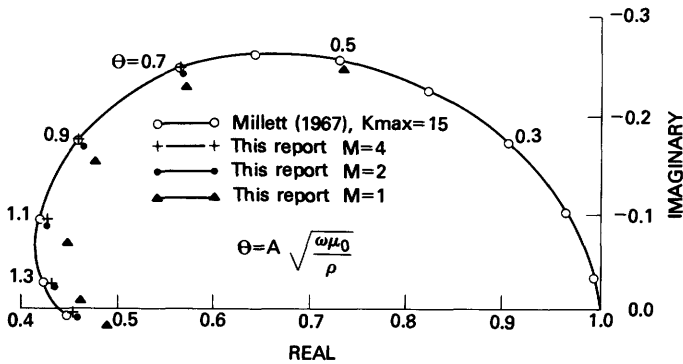


FIGURE 5.—Homogeneous-earth collinear array dipole-dipole electromagnetic coupling plotted in the Cartesian complex plane, showing convergence of the calculations with increasing number of intervals (M) that the dipoles are divided into.

MODEL RESULTS ISOTROPIC EARTH

A comparison of EM coupling for pole-dipole and dipole-dipole arrays for a homogeneous earth is shown in

figure 6. All the results shown have been normalized by the real or dc component. In this form, the pole-dipole curve has a somewhat smaller imaginary amplitude than the dipole-dipole curve; this is due to the diminished \mathbf{Q} term, as the electrodes are moved farther away. However, the effective coupling for the pole-dipole array (especially for PFE's) is greater than for an equivalent (in everything except the J parameter) dipole-dipole configuration. This is because of the increased contribution from the \mathbf{P} or inductive term.

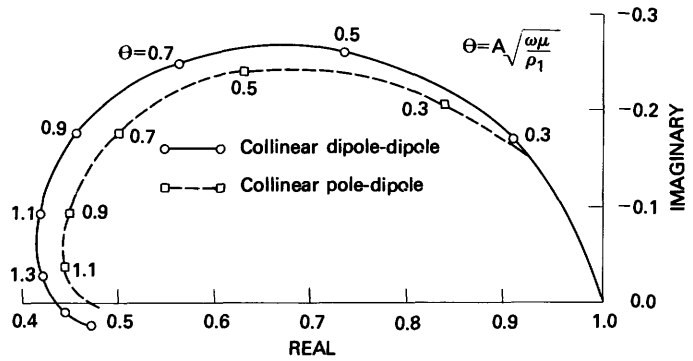


FIGURE 6.—A comparison of homogeneous-earth collinear dipole-dipole coupling with pole-dipole coupling plotted in the Cartesian complex plane.

As mentioned in the introduction, it is a relatively simple matter to obtain PFE's, phase angles, and chargeabilities from the more general, normalized results in the complex plane. This can be demonstrated graphically in figure 7. In this figure, M_1 and M_2 are magnitudes at 0.1 and 1.0 Hz (hertz) respectively, and Φ_1 and Φ_2 are phase angles at the same corresponding frequencies.

Newmont standard chargeabilities can be derived empirically from the phase angle (Φ_1) at 0.1 Hz by multiplying the phase angle in milliradians by a constant factor of 1.2 (Zonge and Wynn, 1975). Loss tangents may be calculated as $L = \tan(\Phi_1 + \pi/2)$.

Figure 2 has already demonstrated the behavior of dipole-dipole coupling for various resistivity contrasts. In general, the phase lag (a negative phase angle) increases rapidly and monotonically for $\rho_1 \leq \rho_2$ in the frequency range of interest. For a resistivity contrast $\rho_1 > \rho_2$, the phase lag initially increases as frequency is increased, but it soon reaches a maximum, decreases, and then crosses over the real axis to a phase lead at the higher frequencies.

Figure 8 shows coupling curves as a function of N , where N is a multiple of dipole spacing. Another example for varying N (in terms of standard IP parameters) is shown in table 1. The results here are similar to those obtained in the field, namely that both magnitudes and phase angles change more rapidly with increasing N -spacing. This gives rise to an apparent layering in field pseudosections, giving increasing coupling contribution with increasing depth or N -spacing.

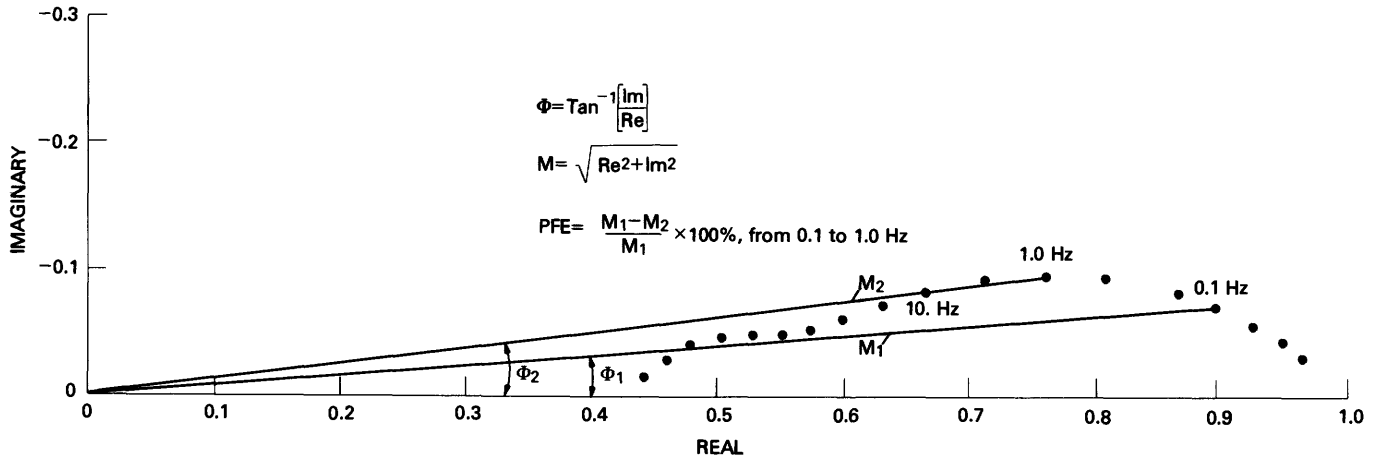


FIGURE 7.—Graphic relationship between the polar coordinate parameters of frequency domain IP and the complex resistivity spectrum represented by the dots in the Cartesian complex plane. PFE is the percent-frequency effect.

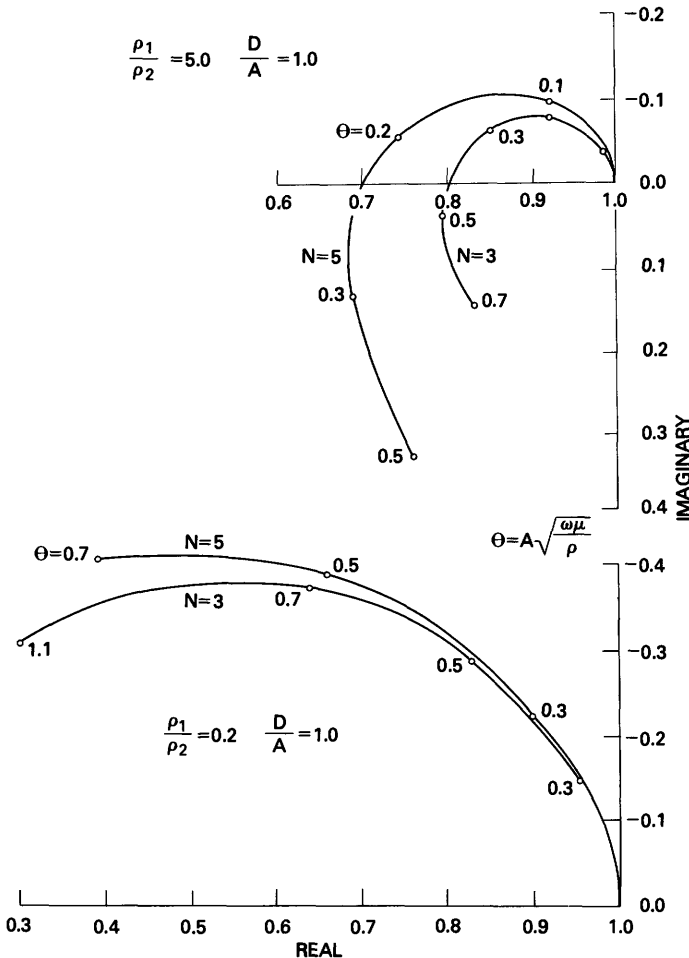


FIGURE 8.—Collinear dipole-dipole EM coupling as a function of N-spacing, for a conductive basement and a resistive basement, plotted in the Cartesian complex plane.

Figure 9 demonstrates the behavior of coupling for the dipole-dipole configuration as a function of D/A (depth to the layer interface). In the limiting case of an infinitely deep

TABLE 1.—IP parameters for a two-layer isotropic earth as a function of N-spacing

[PFE's are for the 0.1-1.0 Hz decade, phase angles are in milliradians, chargeability is in millivolt-seconds per volt, and loss-tangent is dimensionless. A-spacing is 300 m; depth to interface is 60 m; first-layer resistivity is 50 ohm-meters, and second-layer resistivity is 10 ohm-meters]

N	PFE 0.1-1.0 decade	Phase (MRAD)		Charge- ability	Loss- tangent
		1.0 Hz	0.1 Hz		
1	0.8	-31	-3.9	4.7	256
3	7.3	-137	-21	25	47.6
5	17.1	-244	-46	55	21.7
10	43.2	-345	-130	156	7.6

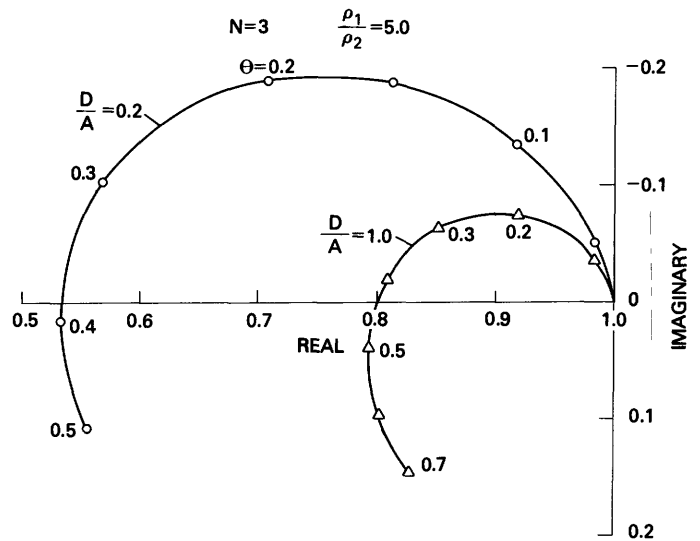


FIGURE 9.—Collinear dipole-dipole EM coupling as a function of D/A (depth to the interface) in the Cartesian complex plane.

or an infinitely shallow interface, the spectra approach the results of figure 6 (the homogeneous earth). An example for a different resistivity contrast, also in terms of standard IP parameters, is shown in table 2.

TABLE 2.—IP parameters for a two-layer isotropic earth as a function of depth to the interface D/A

[Parameters are the same as in table 1. PFE's are for the 0.1-1.0 Hz decade, phase angles are in milliradians, chargeability is in millivolt-seconds per volt, and loss-tangent is dimensionless. A-spacing is 300 m; first-layer resistivity is 50 ohm-meters, and second-layer resistivity is 5 ohm-meters]

D/A	PFE 0.1-1.0 decade	Phase (MRAD)		Charge- ability	Loss- tangent
		1.0 Hz	0.1 Hz		
0.05	15.2	-240	-42	50	24
.10	14.9	-227	-41	49	24
.20	14.3	-202	-38	46	26
1.00	3.71	-41.9	-9.7	11.7	103
1.20	2.55	-35.4	-7.3	8.8	137
1.50	1.76	-33.4	-5.9	7.1	169
2.00	1.28	-35.4	-5.4	6.5	185
5.00	.97	-45.4	-5.6	6.7	179

For a rough check on these theoretical results, a field measurement was made at Willcox Playa, Cochise County, Ariz. The field data are compared in figure 10 with a theoretical plot whose input parameters were derived from a conventional dipole resistivity sounding. The results are within the accuracy of the dipole-sounding inversion and show that the theoretical approach is in fact based on realistic assumptions.

ANISOTROPIC EARTH

The effects of anisotropy on the EM coupling spectra can be measured, where the coefficient of anisotropy for the jth

layer is given as,

$$A_j = \frac{\rho_{jh}}{\rho_{jv}} = \left[\frac{\text{horizontal resistivity}}{\text{vertical resistivity}} \right] \text{ jth layer.}$$

Nine examples of theoretical EM coupling for an anisotropic earth may be found in table 6. An initial examination (figure 11) shows that an anisotropic model for moderate values of A_j will behave as one would intuitively expect. In the case shown here, an anisotropic model chosen somewhere between a homogeneous and an isotropic layered earth model gives results that fit between the homogeneous and isotropic cases.

As the resistive contrasts in the anisotropic layer increase, several features begin to appear that are not obtainable from isotropic earth models. One of these features is an increase in magnitude with increasing frequency in the dc to 0.1 Hz range. This is noticeable in the shorter N-spacings in the earth model of figure 12; it is especially pronounced in the behavior of the Q term. In field measurements this peculiarity would be noticed as negative PFE's. If the earth polarization response were weak enough, this effect could mask the response enough to hide a significant polarization anomaly. The maximum effect in the model of figure 12, however, is only 2 percent on the N=3 curve. This would be significant only if one attempted to compensate by subtracting out isotropic-earth coupling derived from resistivity pseudosections. It should be noted that the phase shifts in the anisotropic case are not greatly different from those of most

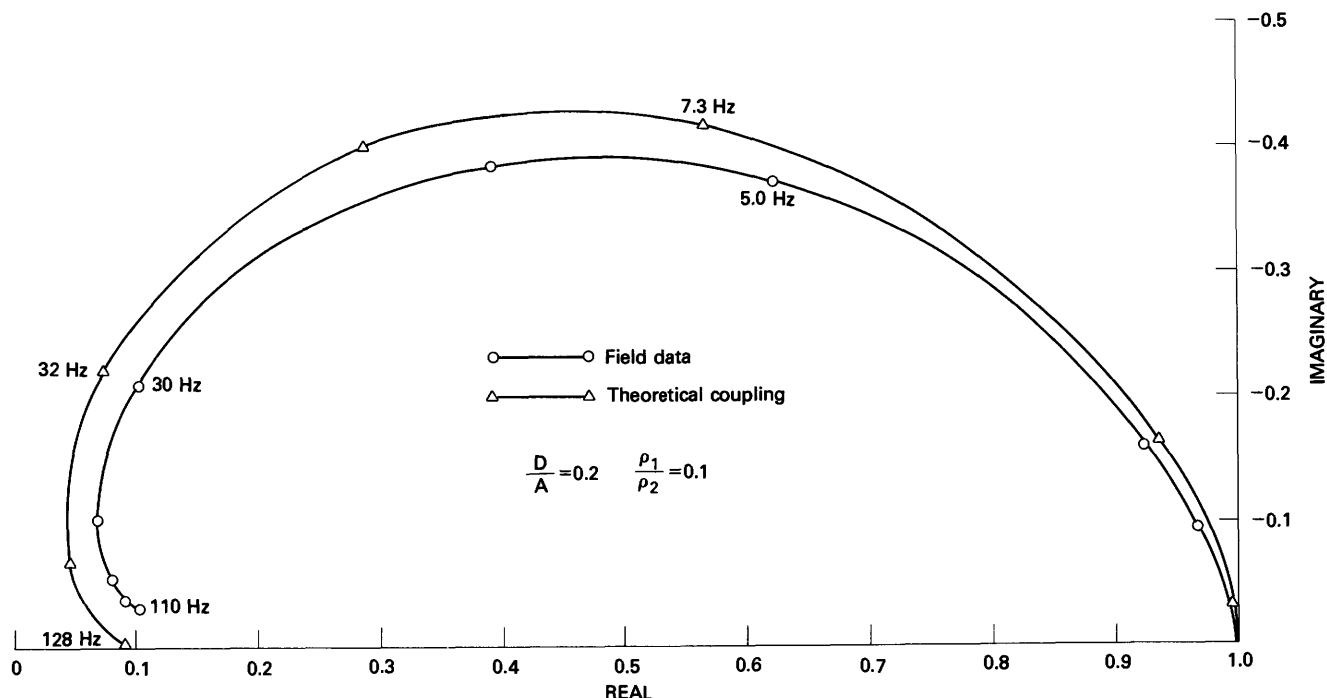


FIGURE 10.—Collinear pole-dipole EM coupling at Willcox Playa, Cochise County, Ariz. Field data are compared with a theoretical model whose parameters were derived from curve-matching dc sounding data. Data plotted in the Cartesian complex plane.

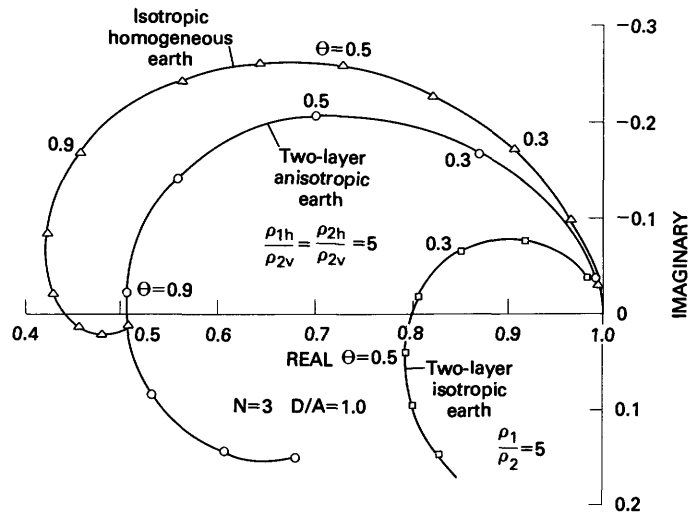


FIGURE 11.—Comparison of anisotropic two-layer-earth EM coupling curve with two isotropic-earth EM coupling curves in the Cartesian complex plane.

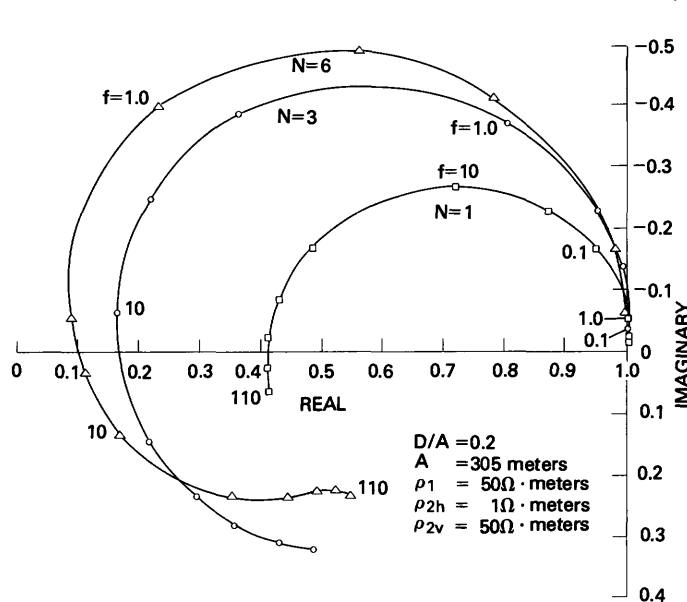


FIGURE 12.—Anisotropic-earth EM coupling curves in the Cartesian complex plane, showing the effect of changing the N-spacing in the models. Note that anisotropy causes increasing magnitudes (and, therefore, negative PFE's) at the lower frequencies.

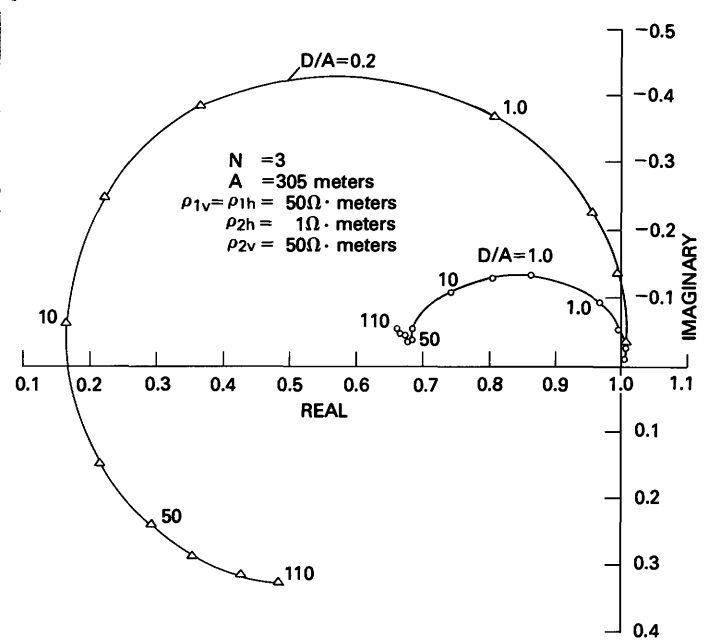


FIGURE 13.—Anisotropic-earth EM coupling curves in the Cartesian complex plane, showing the effect of changing the D/A ratio.

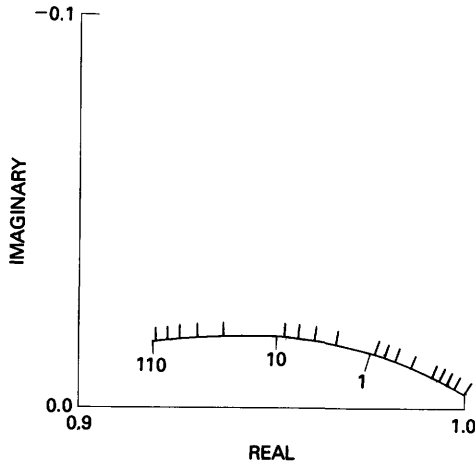
isotropic cases. Anisotropy, therefore, would not be readily identifiable in a purely phase measuring system, or in a time-domain system.

A final feature of interest may be observed in figure 13. In this case, curves for two values of D/A are plotted for a large, fixed anisotropy ratio. Compared with the curve for D/A=0.2, the magnitude and phase changes due to EM coupling diminish as expected in the curve for D/A=1.0. A notchlike behavior appears, however, at the high-frequency end of the D/A=0.2 curve. This high-frequency notch has been observed in field data and has been modeled in other work (Wynn and Zonge, 1975). In the frequency range

normally used in IP (generally less than 1.0 Hz), this notchlike behavior would not be observed unless the earth resistivities were less than that of seawater, which is very unusual, but nevertheless has been encountered.

THE REAL WORLD: ROCK RESPONSE AND COUPLING REMOVAL

Several examples of complex-plane rock spectra and a discussion of the application of coupling removal from field data can be found in Zonge and Wynn (1975) and Wynn and Zonge (1975). In this section the contribution of the rock

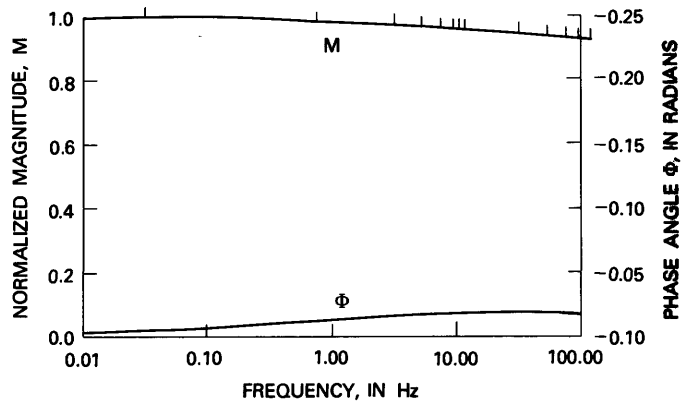


FREQUENCY	COMPONENTS	
	REAL	IMAGINARY
0.01	1.0000	-0.0037
.03	.9976	-.0058
.05	.9959	-.0062
.07	.9939	-.0074
.09	.0028	-.0077
.11	.9931	-.0081
.10	.9927	-.0079
.30	.9863	-.0107
.50	.9826	-.0124
.70	.9798	-.0131
.90	.9776	-.0142
1.10	.9764	-.0152
1.00	.9769	-.0135
3.00	.9663	-.0165
5.00	.9686	-.0175
7.00	.9567	-.0182
9.00	.9537	-.0186
11.00	.9513	-.0189
10.00	.9521	-.0187
30.00	.9376	-.0193
50.00	.9308	-.0186
70.00	.9260	-.0175
90.00	.9226	-.0169
110.00	.9202	-.0161

Apparent resistivity = 1027.3 ohm-meters
Phase at 0.1 Hz = 8.0 milliradians
PFE for 0.1 to 1.0 Hz = 1.5

FIGURE 14.—Weak (barren) rock response spectrum in the Cartesian complex plane, taken from laboratory measurements of a core sample of fresh igneous rock; 0.1, 1.0, and 10 Hz are frequency points and PFE is percent-frequency effect.

response to electromagnetic coupling and a simple coupling removal technique will be discussed. Figures 14 and 15 show an example of the electrical spectral response of a barren igneous rock. This spectrum is called a type "C" response in Zonge and Wynn (1975). The measurement was made in the laboratory in such a manner as to avoid coupling and other

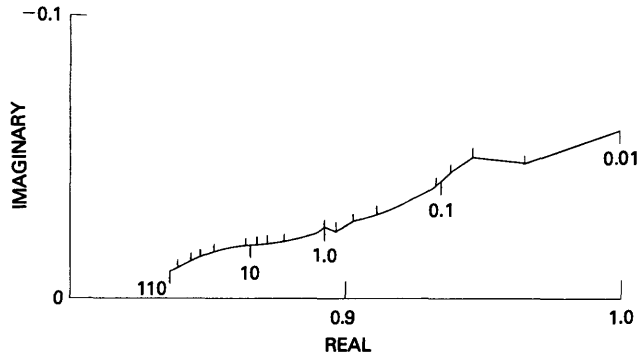


FREQUENCY	MAGNITUDE	PHASE	LOSS-TANGENT
0.01	1.0000	-0.0037	270.7431
.03	.9976	-.0059	170.8859
.05	.9959	-.0062	160.0368
.07	.9939	-.0074	134.3227
.09	.9926	-.0078	128.1578
.11	.9931	-.0081	123.1535
.10	.9927	-.0080	124.8938
.30	.9864	-.0102	92.6125
.50	.9827	-.0126	79.5342
.70	.9799	-.0134	74.7817
.90	.9777	-.0145	68.7416
1.10	.9765	-.0155	64.4400
1.00	.9770	-.0138	72.2468
3.00	.9665	-.0170	58.6813
5.00	.9608	-.0182	54.9466
7.00	.9569	-.0190	52.6324
9.00	.9539	-.0195	51.1506
11.00	.9515	-.0199	50.3428
10.00	.9523	-.0196	50.9916
30.00	.9378	-.0205	48.6609
50.00	.9310	-.0199	50.1678
70.00	.9262	-.0189	52.8972
90.00	.9227	-.0183	54.6585
110.00	.9203	-.0175	57.2592

FIGURE 15.—Weak (barren) rock response spectrum of figure 14, in polar coordinates, plotted in normalized magnitudes and phase angles.

errors. In figures 14 and 16 the triangles (Δ) mark the 0.1, 1.0, and 10 Hz points. Figures 16 and 17 show an example of the electrical spectral response of an altered and mineralized rock; this is a type "A" response as named by Zonge, Wynn, and Young (1976).

These two laboratory data sets can be combined with three theoretical isotropic coupling data sets from table 6 to generate a group of synthetic field results. The data sets were combined by assuming that the second layer was polarizable; to be done rigorously, the coupling should be calculated for a different resistivity for each frequency. The data sets of table 6 that are used here are 2, 3, and 14. A coupling removal technique described by Hallof (1974) can be tested on the resulting data sets. This technique fits a straight line and a quadratic curve to the low-frequency phase angles, and extrapolates the results to give an estimated dc "coupling



COMPONENTS		
FREQUENCY	REAL	IMAGINARY
0.01	0.9983	-0.0590
.03	.9647	-.0480
.05	.9478	-.0505
.07	.9370	-.0439
.09	.9352	-.0408
.11	.9283	-.0399
.10	.9314	-.0389
.30	.9104	-.0291
.50	.9014	-.0267
.70	.8970	-.0237
.90	.9821	-.0252
1.10	.8891	-.0227
1.00	.8905	-.0231
3.00	.8768	-.0195
5.00	.8706	-.0185
7.00	.8668	-.0179
9.00	.8638	-.0177
11.00	.8619	-.0173
10.00	.8625	-.0171
30.00	.8510	-.0149
50.00	.8458	-.0133
70.00	.8423	-.0120
90.00	.8399	-.0111
110.00	.8376	-.0095

Apparent resistivity = 92.1 ohm·meters
 Phase at 0.1 Hz = 41.6 milliradians
 PFE for 0.1 to 1.0 Hz = 4.4

FIGURE 16.—Mineralized- and altered-rock response spectrum, plotted in the Cartesian complex plane; 0.1, 1.0, and 10 Hz are frequency points, and PFE is percent-frequency effect.

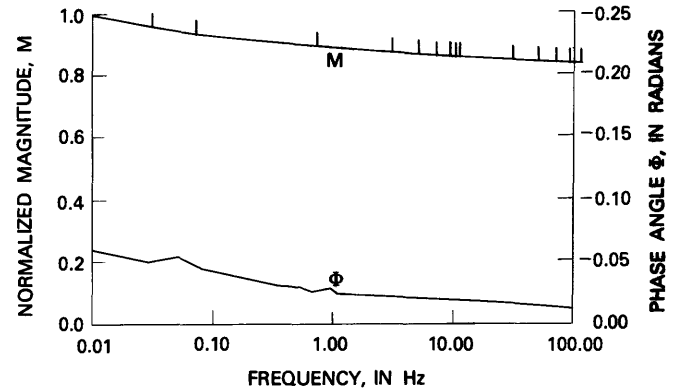
free” phase angle. This extrapolation is accomplished by the following formulas:

$$\text{Extrapolated (linear) phase} = \left[\frac{3}{2} \Phi_{.1} - \frac{1}{2} \Phi_{.3} \right]$$

for .1 and .3 Hz, and

$$\text{Extrapolated (quadratic) phase} = \left[\frac{15}{8} \Phi_{.1} - \frac{5}{4} \Phi_{.3} + \frac{3}{8} \Phi_{.5} \right]$$

for .1, .3, and .5 Hz.



FREQUENCY	MAGNITUDE	PHASE	LOSS-TANGENT
0.01	1.0000	-0.0591	16.9097
.03	.9659	-.0497	20.1062
.05	.9492	-.0532	18.7823
.07	.9380	-.0468	21.3454
.09	.9361	-.0436	22.9272
.11	.9281	-.0430	23.2516
.10	.9322	-.0417	23.9524
.30	.9109	-.0319	31.3272
.50	.9018	-.0296	33.7436
.70	.8963	-.0264	37.8633
.90	.8924	-.0283	35.3569
1.10	.8894	-.0255	39.1500
1.00	.8908	-.0260	38.5017
3.00	.8770	-.0222	45.0012
5.00	.8708	-.0213	46.9744
7.00	.8670	-.0207	48.3297
9.00	.8639	-.0205	48.8417
11.00	.8621	-.0201	49.6880
10.00	.8627	-.0198	50.5681
30.00	.8511	-.0175	57.1147
50.00	.8459	-.0157	63.7213
70.00	.8424	-.0142	70.2471
90.00	.8400	-.0132	75.4765
110.00	.8377	-.0113	88.2485

FIGURE 17.—Mineralized- and altered-rock spectrum of figure 16, in polar coordinates, plotted in normalized magnitudes and phase angles.

Table 3 shows the results of an experimental removal of coupling using Hallof's methods for three theoretical data sets from table 6 and for the three cases of (1) non dispersive rock, (2) type "C" rock, and (3) type "A" rock response added. For comparative purposes the actual phase responses as measured in the laboratory for 0.01 and 0.1 Hz are included. For coupling case 3, the results are quite good, with the dc "coupling free" phase angle falling somewhere between the 0.01 and 0.1 Hz result. Case 3 is theoretical coupling from a two-layer, isotropic, resistive basement environment. As the basement is made more conductive, as in case 2, the coupling removal technique begins to fail, but only for the case in which the inherent rock response included is weak or zero (type "C" or no rock response added). For a sharp resistive contrast, as in coupling case 2, the method fails entirely because the coupling-caused phase

TABLE 3.—Comparison of coupling-removal results with actual laboratory results for three isotropic earth coupling cases

[All data are in milliradians (MRAD)]

	Coupling case			Response of rock only	
	2	3	14	$\phi.01$	$\phi.1$
Coupling removal with no rock response added					
Linear-----	-298	-0.4	-12.0	0.0	0.0
Quadratic-----	-260.4	-.44	-5.8		
Coupling removal with type "C" rock response added					
Linear-----	-304.7	-7.0	-18.6	-3.7	-8.0
Quadratic-----	-266.8	-6.7	-12.0		
Coupling removal with type "A" rock response added					
Linear-----	-345.2	-47.0	-58.6	-59.1	-41.7
Quadratic-----	-310.5	-49.9	-55.2		

shift begins to *increase* rapidly, eventually (by 0.5 Hz in case 2) turning over to a phase-*lead*. This same failure occurs for the homogeneous earth case (though not nearly so seriously) as the earth resistivity becomes small (less than 20 ohm-meters). In any configuration, the coupling becomes less amenable to removal as the N-spacing is increased.

Table 4 shows EM coupling removal tests for three anisotropic models (data sets 28, 29, and 33 of table 6).

TABLE 4.—Comparison of coupling-removal results with laboratory results for three anisotropic earth coupling cases

[All data are in milliradians (MRAD)]

	Coupling case			Response of rock only	
	28	29	33	$\phi.01$	$\phi.1$
Coupling removal with no rock response added					
Linear-----	-1.4	+3.0	-0.3	0.0	0.0
Quadratic-----	-.8	+1.8	-.3		
Coupling removal with type "C" rock response added					
Linear-----	-8.0	-3.7	-6.9	-3.7	-8.0
Quadratic-----	-7.1	-4.4	-6.5		
Coupling removal with type "A" rock response added					
Linear-----	-48.0	-43.7	-46.9	-59.1	-41.7
Quadratic-----	-50.3	-47.6	-49.7		

In the previous section it was pointed out that an anisotropic earth affects principally the magnitude at low frequencies and not the phase angles. This observation is borne out in table 4, where coupling removal for three "typical"

anisotropic models gives results reasonably close to the actual rock response. The conclusion reached here, then, is that an anisotropic earth will not complicate the coupling removal task more than an isotropic earth.

CONCLUSIONS AND COMPUTER RESULTS

Electromagnetic coupling usually affects phase angle measurements more strongly than it does PFE-type measurements, in terms of the relative contribution of coupling as against rock response. This coupling contribution becomes significant when frequencies above 1.0 Hz are used. In one highly conductive environment, in fact, the coupling accounted for more than 75 percent of the phase angle measured at 0.1 Hz. Coupling can, of course, be minimized by using shorter dipole spacings.

The simple coupling removal technique described by Hallof (1974) can be effectively used in possibly half of the field conditions normally encountered. Theoretical modeling shows that introducing anisotropy into the environment can lead to negative PFE's for a collinear dipole-dipole array but does not appreciably alter the phase angles from those obtained over an isotropic earth. Since the method of Hallof utilizes phase angles, this coupling removal technique should work reasonably well in most anisotropic environments.

Further details of the theoretical calculations used in this study may be found in table 5, containing the computer listings, and in table 6, containing examples of electromagnetic coupling for both isotropic and anisotropic-earth models plotted in the Cartesian complex plane.

TABLE 5.—Computer program listings

[MAIN, Controlling main program; COMPAN, Integrating subroutine; READAN, I/O subroutine; ANISOP, Anisotropic P kernel function; ANISOQ, Anisotropic Q kernel function; PDP, Isotropic P kernel function; PDQ, Isotropic Q kernel function; BESJ0, Bessel function of first kind, zeroth order; QG8, Eight-point Gaussian quadrature; QG16, Sixteen-point Gaussian quadrature]

```

MAIN PROGRAM
C PROGRAM TO CALCULATE EM COUPLING FOR A POLE-DIPOLE
C AND DIPOLE-DIPOLE ARRAY OVER A TWO-LAYERED EARTH.
C VAL(1) = N-SPACING
C VAL(2) = A SPACING IN FEET (CONVERTED TO METRIC)
C VAL(3) = RHO-1, IN OHM-METRES
C VAL(4) = RHO-2, IN OHM-METRES
C VAL(5) = D, DEPTH TO THE INTER FACE IN FEET
C (CONVERTED ALSO TO METRIC INTERNALLY)
C VAL(6) = W... IF W=0, IT WILL READ IN THE THETA VALUES,
C OTHERWISE IT GENERATES THE STANDARD FREQUENCY
C SPECTRA ONE MIGHT ANTICIPATE IN THE FIELD,
C (0.1 THRU 110 HZ IN THIS PROGRAM).
C USED LATER IN PROGRAM AS CARRIER FOR THE
C ANGULAR FREQUENCY W (OMEGA).
C VAL(7) = J, THE LENGTH MULTIPLIER FOR THE XMTR DIPOLE
C VAL(8) = M, # OF INTERVALS THAT THE DIPOLES ARE SUB-
C DIVIDED INTO. THIS IS FOR INTEGRATION IN
C EQUATIONS 36 AND 37 OF THE TEXT.
C VAL(9) = RHO-3, SECOND LAYER VERTICAL RESISTIVITY (OHM-M).
C -----
C FOR OPERATION, UTILIZE THE FOLLOWING:
C ASSIGN TTY = 4
C ASSIGN LPT = 5
C
C *****
1 COMPLEX RSLT,Z(16),ZN(16),PTEMP,QTEMP
C
C RSLT IS RESULT FROM INTEGRATION, Z IS IMPEDANCE DERIVED
C FROM P & Q FUNCTIONS, ZN IS NORMALIZED Z, PTEMP & QTEMP
C ARE TEMPORARY STORAGE FOR P & Q CALCULATIONS.
C
2 COMMON /BLK1/ METHOD,VAL(9),NZERO,R,HEADER(20)
3 DIMENSION W(16),TH(16),F(16)
4 WRITE(4,10)
5 WRITE(5,10)

```

TABLE 5.—Computer program listings—Continued

```

6 10 FORMAT(/, ' POLE- AND DIPOLE-DIPOLE ANISO EARTH EM COUPLING ', /
7 1 ' VERSION OF 1 JULY 1976 ', /, 1X, 46(1H*), /)
8 20 CONTINUE
9 CALL READAN
10 IVAL=4
11 C
12 C READIN IS THE GENERALIZED READIN ROUTINE (HIGHLY SIMPLIFIED
13 C HERE) USED TO READ IN THE INPUT PARAMETERS AND STORE THEM
14 C IN THE COMMON ARRAYS.
15 C
16 WRITE(4, 30)
17 30 FORMAT(' INPUT METHOD OF INTEGRATION IN I2 FORMAT: ', /,
18 1 ' 1 = GAUSSIAN QUADRATURE', /, ' 0 = CONVOLUTION')
19 READ(4, 40) METHOD
20 40 FORMAT(I2)
21 IF(METHOD.EQ.0) GO TO 60
22 WRITE(5, 50)
23 50 FORMAT(' INTEGRATION BY GAUSSIAN QUADRATURE')
24 GO TO 80
25 60 WRITE(5, 70)
26 70 FORMAT(' INTEGRATION BY HANKLE TRANSFORM CONVOLUTION')
27 CONTINUE
28 IF(METHOD.EQ.0) GO TO 100
29 WRITE(4, 90)
30 90 FORMAT(' INPUT THE INTEGRATION PARAMETER IVAL IN I2 FORMAT: ')
31 C
32 C IVAL IS THE NUMBER OF INTERVALS INTEGRATED WITH QG16/QG8
33 C BEFORE THE EULER-CONVERGENCE ROUTINE TAKES OVER.
34 C
35 READ(4, 140) IVAL
36 100 CONTINUE
37 C
38 C PROTECT AGAINST ZERO-LENGTH TRANSMITTER:
39 C
40 IF(VAL(7).GT.0) GO TO 110
41 VAL(7)=1.
42 110 CONTINUE
43 C
44 C METRIC CONVERSION:
45 C
46 VAL(2)=VAL(2)*0.30488
47 VAL(5)=VAL(5)*0.30488
48 IF(VAL(1).LE.0.) GO TO 340
49 PI=3.1415926
50 XNORM=1.
51 XMUO=PI*0.0000004
52 A=VAL(2)
53 IF(VAL(6).LE.0.) GO TO 130
54 C
55 C GENERATE THE FREQUENCIES IF THETA.OPTION IGNORED...
56 C
57 W(1)=(0.0001*VAL(3))/(A*A*XMUO)
58 W(2)=.1
59 W(3)=.3
60 W(4)=.5
61 W(5)=1.
62 W(6)=3.
63 W(7)=5.
64 W(8)=10.
65 W(9)=30.
66 W(10)=50.
67 W(11)=70.
68 W(12)=90.
69 W(13)=110.
70 LIM=13
71 DO 120 J=1, LIM
72 F(J)=W(J)
73 W(J)=6.2831852*F(J)
74 TH(J)=A*SQRT(W(J)*XMUO/VAL(3))
75 GO TO 230
76 130 CONTINUE
77 WRITE(4, 150)
78 C
79 C READ IN HOW MANY VALUES OF THETA ARE DESIRED
80 C
81 TH(1)=0.01
82 READ(4, 140) NOTHET
83 140 FORMAT(I2)
84 150 FORMAT(/, ' TYPE IN THE NUMBER OF THETAS, I2 FORMAT: ')
85 WRITE(4, 160)
86 NOTHET=NOTHET+1
87 READ(4, 170) (TH(I), I=2, NOTHET)
88 160 FORMAT(/, ' INPUT VALUES IN F10.5 FORMAT: ', /)
89 170 FORMAT(15(F10.5, /))
90 C
91 C FOLLOWING SECTION WILL TRUNCATE THETA ARRAY IF IT
92 C ENCOUNTERS A ZERO IN IT, AND RESET LIM AUTOMATICALLY
93 C
94 LIM=16
95 DO 180 I=2, 16
96 IF(TH(I).GT.0.) GO TO 180
97 LIM=I-1
98 GO TO 190
99 180 CONTINUE
100 190 CONTINUE
101 IF(TH(2).GT.0.) GO TO 210
102 LIM=9
103 DO 200 K=1, 8
104 KP=K+1
105 XKP=FLOAT(KP)
106 TH(KP)=(XKP-2.)*0.2+0.1
107 200 CONTINUE
108 C
109 C CONVERT THETAS TO ANGULAR FREQUENCY...
110 C
111 DO 220 J=1, LIM
112 W(J)=(TH(J)*TH(J)*VAL(3))/(A*A*XMUO)
113 220 CONTINUE
114 WRITE(4, 240) (HEADER(I), I=1, 20)
115 WRITE(5, 240) (HEADER(I), I=1, 20)
116 240 FORMAT(1X, 62(1H*), /, 1X, 1H*, 20A3, 1H*, /, 1X, 62(1H*))

```

TABLE 5.—Computer program listings—Continued.

```

87 WRITE(4, 250)
88 WRITE(5, 250)
89 250 FORMAT(/, ' N A RHO-1 RHO-2 DEPTH',
90 1 ' W J M RHO-3 ', /, 9(7H *****))
91 WRITE(4, 260) (VAL(J), J=1, 9)
92 WRITE(5, 260) (VAL(J), J=1, 9)
93 260 FORMAT(2F7.0, 2F7.1, 4F7.0, F7.1)
94 WRITE(4, 270)
95 WRITE(5, 270)
96 270 FORMAT(26H RESULTS ARE AS FOLLOWS....
97 1 /, 1X, 5HTHETA, ' FREQ REAL IMAG PREAL PIMAG',
98 2 20H QREAL QIMAG /, 16H ***** *****,
99 3 2X, 4H*****, 4X, 4H*****, 2X, 2(4X, 4H*****), 2X, 2(4X, 4H*****))
100 C
101 C CALCULATE THE IMPEDANCES, Z...
102 C
103 DO 300 I=1, LIM
104 VAL(6)=W(I)
105 SKD=SQRT(2.*VAL(3)/(VAL(6)*PI*0.0000004))
106 C
107 C SKD IS THE SKIN-DEPTH USED IN GENERALIZING THE LINEAR
108 C VARIABLES TO MAKE THEM DIMENSIONLESS.
109 C
110 Z(I)=CMPLX(0., 0.)
111 IF(W(I).LE.0.) GO TO 300
112 MM=FIX(VAL(8))
113 XMM=VAL(8)
114 MJ=FIX(VAL(7)*VAL(8))
115 C
116 C MM IS THE NUMBER OF INTERVALS THAT THE RECEIVER DIPOLE IS
117 C DIVIDED INTO, AND MJ IS THE NUMBER OF INTERVALS THAT THE
118 C TRANSMITTER IS DIVIDED INTO FOR THE DOUBLE SUMMATION.
119 C
120 DO 290 L=1, MJ
121 DO 280 H=1, MM
122 XL=FLOAT(L)
123 XM=FLOAT(M)
124 R=(1.+VAL(1)+(XL-XM)/XMM)*A
125 C
126 C R IS THE DISTANCE BETWEEN SEGMENTS OF THE DIPOLES
127 C BEING INTEGRATED OVER.
128 109 CALL COMPAN(RSLT, 1, IVAL)
129 C
130 C FROM ZERO TO INFINITY;... 1 MEANS IT USES ANISOP, 2 MEANS
131 C IT USES ANISOQ FOR THE KERNEL FUNCTION. RSLT IS RETURNED.
132 110 Z(I)=Z(I)+RSLT
133 111 CONTINUE
134 112 CONTINUE
135 C
136 C CONTRIBUTION FROM DOUBLE SUM OF P:
137 113 Z(I)=Z(I)*2.*PI*A*A*A/(VAL(3)*XMM*XMM)
138 C
139 C IT HAS JUST BEEN NORMALIZED BY Z(DC).
140 C
141 PTEMP=Z(I)
142 CALL COMPAN(RSLT, 2, IVAL)
143 C
144 C CONTRIBUTION FROM Q:
145 116 QTEMP=RSLT*2.*PI*A/VAL(3)
146 117 Z(I)=Z(I)+QTEMP
147 C
148 C CALCULATE NORMALIZED IMPEDANCES ZN...
149 C
150 IF(L.LE.1) XNORM=REAL(Z(I))
151 ZN(I)=Z(I)/XNORM
152 PTEMP=PTEMP/XNORM
153 QTEMP=QTEMP/XNORM
154 F(I)=W(I)/6.2831852
155 C
156 C OUTPUT THE RESULT...
157 123 WRITE(4, 310) TH(I), F(I), ZN(I), PTEMP, QTEMP
158 124 WRITE(5, 310) TH(I), F(I), ZN(I), PTEMP, QTEMP
159 125 CONTINUE
160 300 310 FORMAT(F7.3, F7.1, 2F8.4, 2X, 2F8.4, 2X, 2F8.4)
161 WRITE(4, 320) XNORM
162 128 WRITE(5, 320) XNORM
163 320 FORMAT(/, ' NORMALIZING FACTOR = ', E12.4)
164 130 WRITE(4, 330)
165 131 WRITE(5, 330)
166 132 330 FORMAT(1H1, /)
167 133 GO TO 20
168 134 STOP
169 135 END

```

COMPAN SUBROUTINE

```

1 SUBROUTINE COMPAN(RSLT, IFCN, IVAL)
2 C
3 C GENERALIZED INTEGRATION SUBROUTINE
4 C
5 C COMPLEX ANISOP, ANISOQ, ANCONP, ANCONQ, ZHANKO
6 C EXTERNAL ANISOP, ANISOQ, ANCONP, ANCONQ
7 C COMPLEX SSUM, GSUM, ESUM, SUMC, TEM, Y, SEVEN, SODD, FX, AMN, AMP, RSLT
8 C COMMON /BLK1/ METHOD, VAL(9), NZERO, R, HEADER(20)
9 C DIMENSION SUMC(7), Y(193)
10 C DIMENSION V(4), ZERO(25)
11 C DATA ZERO/2.40482555, 5.52007811, 8.65372791, 11.7915344,
12 1 14.9309177, 18.0710639, 21.2116366, 24.3524715,
13 2 27.4934791, 30.6346064, 33.7758202, 36.9170983,
14 3 40.0584257, 43.1997917, 46.3411893, 49.4826098,
15 4 52.6240518, 55.7655107, 58.9069839, 62.0484691,
16 5 65.1899648, 68.3314693, 71.4729816, 74.6145006,
17 6 77.7560256/
18 C DATA ICALLD/1/
19 IF(ICALLD.EQ.1) TEM=CMPLX(0., 0.)

```

TABLE 5.—Computer program listings—Continued.

```

11 ICALLD=ICALLD+10
12 IF (IVAL.EQ.0) IVAL=3
13 NZERO=1
14 PI=3.1415926
15 MAX=8
16 SSUM=TEM
17 GSUM=TEM
18 ESUM=TEM
19 RSLT=TEM
20 NN=0
21 IF (METHOD.EQ.0) GO TO 320
C THE GAUSSIAN INTEGRATION METHOD:
C
C SIMPSON INTEGRATION OVER FIRST INTERVAL OF JO
C
22 DO 10 J=1,6
23 10 SUMC(J)=TEM
24 DO 20 L=1,193
25 20 Y(L)=TEM
26 J=0
27 30 J=J+1
28 NN=6*(2**J)
29 H=(2.4048256)/NN
30 IF (IFCTN-1) 40,40,50
31 40 Y(1)=ANISOP(0.0)
32 GO TO 60
33 50 Y(1)=ANISOQ(0.0)
34 60 CONTINUE
35 NP=NN+1
36 DO 90 I=2,NP
37 XI=FLOAT(I-1)
38 IF (IFCTN-1) 70,70,80
39 70 Y(I)=ANISOP(H*XI)
40 GO TO 90
41 80 Y(I)=ANISOQ(H*XI)
42 90 CONTINUE
43 SEVEN=TEM
44 DO 100 K=2,NN,2
45 100 SEVEN=SEVEN+4.*Y(K)
46 SODD=TEM
47 NM=NN-1
48 DO 110 K=3,NM,2
49 110 SODD=SODD+2.*Y(K)
C THE RESULT...
C SUMC(J)=(H/3.)*(Y(1)+SODD+SEVEN+Y(NP))
C TEST SECTION...
51 IF (J.LE.1) GO TO 30
52 FRAC1=CABS(SUMC(J)-SUMC(J-1))
53 FRAC2=0.00001*CABS(SUMC(J))
54 IF (FRAC1.LE.FRAC2) GO TO 120
55 IF (J.LT.5) GO TO 30
56 120 SSUM=SUMC(J)
57 RSLT=RSLT+SSUM
C
C GAUSSIAN 8-OR-16 POINT INTEGRATION OVER NEXT IVAL INTERVALS...
C
58 DO 190 L=1,IVAL
59 NZERO=L
60 IF (L.LE.4) GO TO 150
61 IF (IFCTN-1) 130,130,140
62 130 CALL QG8(ZERO(L),ZERO(L+1),ANISOP,GSUM)
63 GO TO 180
64 140 CALL QG8(ZERO(L),ZERO(L+1),ANISOQ,GSUM)
65 GO TO 180
66 150 IF (IFCTN-1) 160,160,170
67 160 CALL QG16(ZERO(L),ZERO(L+1),ANISOP,GSUM)
68 GO TO 180
69 170 CALL QG16(ZERO(L),ZERO(L+1),ANISOQ,GSUM)
70 180 RSLT=RSLT+GSUM
71 190 CONTINUE
72 EPS=0.00001*CABS(RSLT)
C
C EULER TRANSFORMATION TO FORCE CONVERGENCE OF SERIES...
C
73 NZERO=NZERO+1
74 DO 200 L=1,193
75 200 Y(L)=TEM
76 IF (MAX.LE.0) GO TO 310
77 I=1
78 M=1
79 XL=ZERO(NZERO)
80 XU=ZERO(NZERO+1)
C XL=LOWER BOUND, XU=UPPER BOUND FOR GAUSSIAN QUADRATURE...
81 IF (IFCTN-1) 220,220,210
82 210 CALL QG8(XL,XU,ANISOQ,FX)
83 GO TO 230
84 220 CALL QG8(XL,XU,ANISOP,FX)
85 230 CONTINUE
86 Y(1)=FX
87 ESUM=Y(1)*.5
88 J=0
89 I=I+1
90 IF (I.GT.MAX) GO TO 310
91 NZERO=NZERO+1
92 XL=ZERO(NZERO)
93 XU=ZERO(NZERO+1)
94 IF (IFCTN-1) 270,270,260
95 260 CALL QG8(XL,XU,ANISOQ,FX)
96 GO TO 280
97 270 CALL QG8(XL,XU,ANISOP,FX)
98 280 AMN=FX
99 DO 290 K=1,M
100 AMP=(AMN+Y(K))*5
101 Y(K)=AMN
102 290 AMN=AMP
103 IF (CABS(AMN).GE.CABS(Y(M))) GO TO 300
104 IF (M.GE.15) GO TO 300
105 M=M+1
106 Y(M)=AMN
107 AMN=.5*AMN
108 300 ESUM=ESUM+AMN

```

TABLE 5.—Computer program listings—Continued.

```

109 IF (CABS(AMN).GT.EPS*CABS(ESUM)) GO TO 240
110 J=J+1
111 IF (J.LT.5) GO TO 250
112 310 CONTINUE
113 RSLT=RSLT+ESUM
114 RETURN
115 320 CONTINUE
C CONVOLUTION/HANKLE TRANSFORM METHOD:
116 IF (IFCTN.EQ.2) GO TO 330
C
C P-FUNCTION CONVOLUTION
C
117 SKD=SQRT(2.*VAL(3)/(VAL(6)*PI*0.0000004))
118 R=R/SKD
119 RSLT=ZHANKO(ALOG(R),ANCONP,0.0001,L)/R
120 RETURN
121 330 CONTINUE
C
C Q-FUNCTION CONVOLUTION
C
122 V(1)=(VAL(1)+VAL(7))*VAL(2)
123 V(2)=VAL(1)*VAL(2)
124 V(3)=(VAL(1)+VAL(7)+1.)*VAL(2)
125 V(4)=(VAL(1)+1.)*VAL(2)
126 DO 340 K=1,4
127 R=V(K)/SKD
128 Y(K)=ZHANKO(ALOG(R),ANCONQ,0.0001,L)/R
129 340 CONTINUE
130 RSLT=Y(1)-Y(2)-Y(3)+Y(4)
131 RETURN
132 END
READAN SUBROUTINE
1 SUBROUTINE READAN
C
C GENERALIZED I/O SUBROUTINE
C
2 COMMON /BLK1/ VAL(9),NZERO,R,HEADER(20)
3 WRITE(4,10)
4 10 FORMAT(/,' GIVE ME A TITLE')
5 READ(4,20)(HEADER(J),J=1,20)
6 20 FORMAT(20A3)
7 WRITE(4,30)
8 30 FORMAT(/,' INPUT THE NINE VARIABLES ',/,
9 1 N A RHO-1 RHO-2 DEPTH TH:W=D J M RHO-3'
10 2 /,9(7H *****))
11 READ(4,40)(VAL(J),J=1,9)
12 40 FORMAT(9F7.0)
13 RETURN
14 50 STOP
15 END
ANISOP FUNCTION
1 COMPLEX FUNCTION ANISOP(X)
C ANISOTROPIC TWO-LAYERED INDUCTIVE FUNCTION.
2 COMPLEX U,V,DELP,DELOP,DELIP,DELOPP,DELIPP,W
3 COMPLEX F1,G1,XI2,CC,XXKSK,WKKAN,XKON
4 COMMON /BLK1/ VAL(9),NZERO,R,HEADER(20)
5 PI=3.1415926
6 SKD=SQRT(2.*VAL(3)/(VAL(6)*PI*0.0000004))
7 XK=VAL(3)/VAL(4)
8 AM=VAL(4)/VAL(9)
9 D=VAL(5)*2./SKD
10 IF (X-.0001) 10,20,20
11 10 X=0.0001
12 20 CONTINUE
13 RVAL=BESJO(X)
14 BLM=R/SKD
15 G=X/BLM
16 G2=G*G
17 XI2=2.*CMPLX(0.,1.)
18 U=CSQRT(G2+XI2)
19 CC=CEXP(-U*D)
20 SKD2=SKD*SKD
21 SKD3=SKD2*SKD
22 XKAN=XK*AN
23 V=CSQRT(G2+XI2*XK)
24 W=CSQRT(G2+XI2*XKAN)
25 DELOPP=G*XI2/SKD3
26 DELOP=DELOPP
27 XXKSK=XI2*XK/SKD3
28 WKKAN=W/XKAN
29 DELIP=XXKSK*(U+WKKAN)
30 DELIPP=XXKSK*(U-WKKAN)
31 DELP=(G+U)*(U+V)+(G-U)*(U-V)*CC
32 XKON=VAL(6)*0.0000001*G*SKD2/DELP
33 F1=XKON*(U+V)
34 G1=XKON*(U-V)*CC
35 ANISOP=(XI2/SKD3)*(F1+G1)*RVAL/BLM
36 RETURN
37 END
ANISOQ FUNCTION
1 COMPLEX FUNCTION ANISOQ(X)
C ANISOTROPIC TWO-LAYERED CONDUCTIVE FUNCTION.
2 COMPLEX U,V,XNUM,Q,DELP,DELOP,DELIP,DELOPP,DELIPP,W
3 COMPLEX DENOM,F1,G1,P1,Q1,XI2,CC,XXKSK,WKKAN,XKON
4 COMMON /BLK1/ VAL(9),NZERO,R,HEADER(20)
5 DIMENSION Y(4),Q(4)
6 PI=3.1415926
7 SKD=SQRT(2.*VAL(3)/(VAL(6)*PI*0.0000004))
8 Y(1)=(VAL(1)+VAL(7))*VAL(2)/SKD
9 Y(2)=VAL(1)*VAL(2)/SKD
10 Y(3)=(VAL(1)+VAL(7)+1.)*VAL(2)/SKD
11 Y(4)=(VAL(1)+1.)*VAL(2)/SKD
12 XK=VAL(3)/VAL(4)

```

TABLE 5.—Computer program listings—Continued.

```

13 AN=VAL(4)/VAL(9)
14 XI2=2.*CMPLX(0.,1.)
15 D=VAL(5)*2./SKD
16 IF(X=0.0001) 10,20,20
17 10 X=0.0001
18 20 CONTINUE
19 RVAL=BESJO(X)
20 DO 30 I=1,4
21 B=Y(I)
22 G=X/B
23 G2=G*G
24 U=CSQRT(G2+XI2)
25 CC=CEXP(-U*D)
26 XKAN=KK*AN
27 SKD2=SKD*SKD
28 SKD3=SKD2*SKD
29 V=CSQRT(G2+XI2*XK)
30 W=CSQRT(G2+XI2*XKAN)
31 DELOPP=G*XI2/SKD3
32 DELOP=DELOPP
33 XXKSK=XI2*XK/SKD3
34 WKKAN=W/XKAN
35 DELIP=XXKSK*(U+WKKAN)
36 DELIPP=XXKSK*(U-WKKAN)
37 XNUM=(G*XI2)/SKD3
38 DENOM=DELIPP*DELOPP*CC+DELOP*DELIP
39 DELP=(G+U)*(U+V)+(G-U)*(U-V)*CC
40 XKON=VAL(6)*0.000001*G*SKD2/DELP
41 F1=XKON*(U+V)
42 G1=XKON*(U-V)*CC
43 P1=XNUM*(-(F1+G1)*DELIP+(XK-1.)*(F1*CC+G1)*DELOPP)/DENOM
44 Q1=XNUM*(1.-XK)*(F1*CC+G1)*DELOP-(F1+G1)*DELIPP*CC/DENOM
45 Q(I)=(F1+G1-(U/G)*(P1-Q1))*RVAL/(B*SKD)
46 30 CONTINUE
47 ANISOQ=Q(1)-Q(2)-Q(3)+Q(4)
48 RETURN
49 END
    
```

PDP FUNCTION

```

1 COMPLEX FUNCTION PDP(X)
C
C
C
2 COMPLEX DEL3,DEL, XI,U,V,CUD,D
3 COMMON /BLK1/ ZERO(35),VAL(8),NZERO,R,HEADER(20)
4 PI=3.1415926
5 SKD=SQRT(2.*VAL(3)/(VAL(6)*PI*0.0000004))
6 XK=VAL(3)/VAL(4)
7 IF(X.LE.0.00005) X=0.00005
8 RVAL=BESJO(X)
9 BLM=R/SKD
10 G=X/BLM
11 G2=G*G
12 D=VAL(5)*2./SKD
13 XI=CMPLX(0.,2.)
14 U=CSQRT(G2+XI)
15 V=CSQRT(G2+XI*XK)
16 CUD=(U-V)*CEXP(-U*D)
17 DEL3=U+V+CUD
18 DEL=(G+U)*(U+V)+(G-U)*CUD
19 PDP=((DEL3/DEL)*RVAL*X)/(BLM*BLM)
20 RETURN
21 END
    
```

PDQ FUNCTION

```

1 COMPLEX FUNCTION PDQ(X)
C
C
C
2 COMPLEX XI,U,V,DEL,DEL1,DEL2,DEL3,Q(4)
3 COMPLEX UKK,CUD,UMV,UKKV,UKKPV,D
4 COMMON /BLK1/ ZERO(35),VAL(8),NZERO,R,HEADER(20)
5 DIMENSION Y(4)
6 PI=3.1415926
7 SKD=SQRT(2.*VAL(3)/(VAL(6)*PI*0.0000004))
8 VSKD=VAL(2)/SKD
9 Y(1)=(VAL(1)+VAL(7))*VSKD
10 Y(2)=VAL(1)*VSKD
11 Y(3)=(VAL(1)+VAL(7)+1.)*VSKD
12 Y(4)=(VAL(1)+1.)*VSKD
13 XK=VAL(3)/VAL(4)
14 XI=CMPLX(0.,2.)
15 D=VAL(5)*2./SKD
16 IF(X.LE.0.00005) X=0.00005
17 RVAL=BESJO(X)
18 DO 10 I=1,4
19 B=Y(I)
20 G=X/B
21 G2=G*G
22 U=CSQRT(XI+G2)
23 V=CSQRT(XI*XK+G2)
24 UKK=U*XK
25 CUD=CEXP(-U*D)
26 UMV=(U-V)*CUD
27 UKKV=(UKK-V)*CUD
28 UKKPV=UKK+V
29 DEL1=UKKPV+UKKV
30 DEL2=(G+U)*UKKPV+(G-U)*UKKV
31 DEL3=U+V+UMV
32 DEL=(G+U)*(U+V)+(G-U)*UMV
33 Q(I)=(4.*(1.-XK)*G*U*U*CUD+DEL2*DEL3)*RVAL/(B*DEL*DEL1)
34 10 CONTINUE
35 PDQ=Q(1)-Q(2)-Q(3)+Q(4)
36 PDQ=Q(AC)-Q(BC)-Q(AD)+Q(BD)
37 RETURN
38 END
    
```

TABLE 5.—Computer program listings—Continued

BESJO FUNCTION

```

1 FUNCTION BESJO(X)
C
C
C
2 COMPUTES J0(X) FOR REAL X
3
4 IF(X.GT.3.) GO TO 10
5 Y=X/3.
6 Y2=Y*Y
7 Y4=Y2*Y2
8 Y8=Y4*Y4
9 Y12=Y8*Y2
10 Y12=Y10*Y2
11 BESJO=1.-2.2499997*Y2+1.2656208*Y4-0.3163866*Y6
12 +0.0444479*Y8-0.0039444*Y10+0.0002100*Y12
13 GO TO 20
14 20 Z=3./X
15 Z2=Z*Z
16 Z3=Z2*Z
17 Z4=Z2*Z2
18 Z5=Z3*Z2
19 Z6=Z3*Z3
20 F0=0.79788456-0.00000077*Z-0.00552740*Z2-0.00009512*Z3
21 +0.00137237*Z4-0.00072805*Z5+0.00014476*Z6
22 THETA=X-0.78539816-0.04166397*Z-0.00003954*Z2+0.00262573*Z3
23 -0.00054125*Z4-0.00029333*Z5+0.00013558*Z6
24 BESJO=F0*COS(THETA)/SQRT(X)
25 20 RETURN
26 END
    
```

QG8 SUBROUTINE

```

1 SUBROUTINE QG8(XL,XU,FCT,Y)
C
C
C
2 8-POINT GAUSSIAN QUADRATURE, ADAPTED FROM IBM SSP.
3 COMPLEX FCT,Y
4 A=.5*(XU+XL)
5 B=XU-XL
6 C=.4801449*B
7 Y=.05061427*(FCT(A+C)+FCT(A-C))
8 C=.3983332*B
9 Y=Y+.1111905*(FCT(A+C)+FCT(A-C))
10 C=.2627662*B
11 Y=Y+.1568533*(FCT(A+C)+FCT(A-C))
12 C=.09171732*B
13 Y=Y+.1813419*(FCT(A+C)+FCT(A-C))
14 RETURN
15 END
    
```

QG16 SUBROUTINE

```

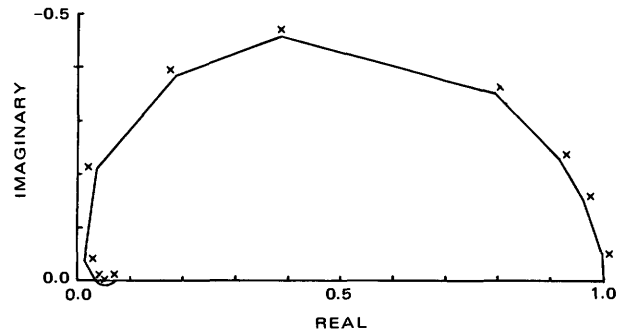
1 SUBROUTINE QG16(XL,XU,FCT,Y)
C
C
C
2 16-POINT GAUSSIAN QUADRATURE, ADAPTED FROM IBM SSP.
3 COMPLEX FCT,Y
4 A=.5*(XU+XL)
5 B=XU-XL
6 C=.494700467496*B
7 Y=.0135762297059 *(FCT(A+C)+FCT(A-C))
8 C=.472287511537*B
9 Y=Y+.031126761969 *(FCT(A+C)+FCT(A-C))
10 C=.43281560119*B
11 Y=Y+.0475792558412 *(FCT(A+C)+FCT(A-C))
12 C=.37702204178*B
13 Y=Y+.0623144856278 *(FCT(A+C)+FCT(A-C))
14 C=.308938122201*B
15 Y=Y+.0747979944083 *(FCT(A+C)+FCT(A-C))
16 C=.22900838829*B
17 Y=Y+.0845782596975 *(FCT(A+C)+FCT(A-C))
18 C=.14080177539*B
19 Y=Y+.0913017075225 *(FCT(A+C)+FCT(A-C))
20 C=.0475062549188*B
21 Y=Y+.0947253052275 *(FCT(A+C)+FCT(A-C))
22 RETURN
23 END
    
```

TABLE 6.—Examples with index of electromagnetic coupling for isotropic and anisotropic two-layer earth models

[N, dipole separation in terms of dipole length A; D/A, depth to dipole-length ratio; ρ_1/ρ_{2h} , resistivity ratio; J, transmitter-length multiplier; A_2 , anisotropy ratio; IMAG, imaginary axis; REAL, real axis; ρ_1 , resistivity of layer 1; ρ_2 , resistivity of layer 2; ρ_3 , resistivity of layer 3; W, angular frequency; M, dipole multiplier; THETA, dimensionless coupling parameter; FREQ, frequency= $W/2\pi$; PREAL, real component of the inductive function; PIMAG, imaginary component of the inductive function; QREAL, real component of the conductive function; QIMAG, imaginary component of the conductive function. Tabulated data are facsimiles of computer printout]

Example	N	D/A	ρ_1/ρ_{2h}	J	A_2
1	3	0.30	0.01	5	1
2	6	.50	50.0	1	1
3	6	.50	.02	1	1
4	6	.50	1.00	1	1
5	6	.50	20.0	1	1
6	1	.50	.04	1	1
7	1	.50	.02	1	1
8	2	.30	.11	5	1
9	3	.10	20.0	1	1
10	3	.20	.10	1	1
11	3	.05	10.0	1	1
12	3	.10	5.0	1	1
13	3	.10	10.0	1	1
14	3	.20	10.0	1	1
15	3	1.00	10.0	1	1
16	3	1.20	10.0	1	1
17	3	1.50	10.0	1	1
18	3	2.00	10.0	1	1
19	3	5.00	10.0	1	1
20	1	.20	5.0	1	1
21	5	.20	5.0	1	1
22	10	.20	5.0	1	1
23	1	.20	.1	1	1
24	1	.20	.01	1	1
25	5	.20	.01	1	1
26	3	.2	5.0	1	.20
27	3	.2	50.	1	.02
28	3	.2	1.0	1	50.0
29	1	.2	50.	1	.02
30	6	.2	50.	1	.02
31	3	1.0	50.	1	.02
32	3	.2	500.	1	.002
33	3	.03	.01	1	20.0
34	3	.03	.001	5	50.0

Example 1:



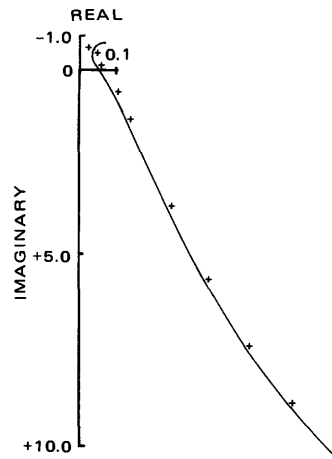
N	A	RHO-1	RHO-2	DEPTH	W	J	M
3.	305.	1.0	100.0	91	1.	5.	2.

RESULTS ARE AS FOLLOWS...

THETA	FREQ	REAL	IMAG	PREAL	PIMAG	QREAL	QIMAG
0.01	0.0	1.0000	0.0015	-0.0000	-0.0005	1.0000	0.0020
0.27	0.1	0.9961	-0.0556	-0.0110	-0.0513	1.0071	-0.0043
0.47	0.3	0.9637	-0.1485	-0.0580	-0.1238	1.0217	-0.0247
0.61	0.5	0.9201	-0.2229	-0.1159	-0.1661	1.0360	-0.0568
0.86	1.0	0.7952	-0.3505	-0.2534	-0.1874	1.0487	-0.1630
1.48	3.0	0.3880	-0.4589	-0.4300	0.0639	0.8180	-0.5228
1.92	5.0	0.1851	-0.3853	-0.3180	0.2236	0.5031	-0.6089
2.71	10.0	0.0363	-0.2125	-0.0724	0.2096	0.1087	-0.4221
4.69	30.0	0.0144	-0.0377	-0.0235	0.0227	0.0379	-0.0604
6.06	50.0	0.0331	-0.0014	-0.0426	0.0009	0.0757	-0.0023
7.17	70.0	0.0486	0.0080	-0.0521	-0.0037	0.1006	0.0117
8.13	90.0	0.0578	0.0082	-0.0572	-0.0043	0.1150	0.0125
8.98	110.0	0.0624	0.0061	-0.0599	-0.0037	0.1223	0.0097

NORMALIZING FACTOR = -0.5509E+00

Example 2:



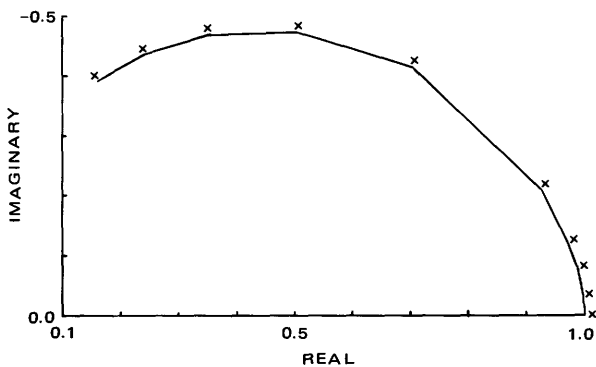
N	A	RHO-1	RHO-2	DEPTH	W	J	M
6.	305.	50.0	1.0	152.	1.	1.	2.

RESULTS ARE AS FOLLOWS...

THETA	FREQ	REAL	IMAG	PREAL	PIMAG	QREAL	QIMAG
0.01	0.0	1.0000	-0.1475	-0.1054	-0.2048	1.1054	0.0572
0.04	0.1	0.8620	-0.1801	-0.2490	-0.3183	1.1110	0.1382
0.07	0.3	0.6464	-0.0141	-0.5470	-0.4033	1.1934	0.3892
0.09	0.5	0.6320	0.1701	-0.6747	-0.4051	1.3067	0.5752
0.12	1.0	0.7663	0.4288	-0.7901	-0.4482	1.5564	0.8770
0.21	3.0	1.0748	0.8215	-1.0068	-0.8132	2.0816	1.6347
0.27	5.0	1.2434	1.1481	-1.1777	-1.1336	2.4211	2.2816
0.38	10.0	1.5818	1.8602	-1.5095	-1.8278	3.0913	3.6881
0.66	30.0	2.6502	4.1755	-2.5495	-4.1003	5.1997	8.2758
0.86	50.0	3.6901	6.1254	-3.5600	-6.0224	7.2501	12.1478
1.01	70.0	4.7955	7.8439	-4.6354	-7.7220	9.4309	15.5660
1.15	90.0	5.9764	9.3666	-5.7860	-9.2330	11.7624	18.5995
1.27	110.0	7.2238	10.7071	-7.0047	-10.5685	14.2285	21.2756

NORMALIZING FACTOR = -0.1113E-03

Example 3:



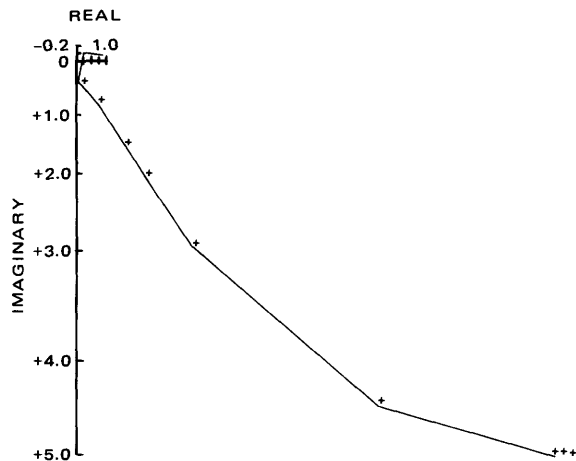
N	A	RHO-1	RHO-2	DEPTH	W	J	M
6.	305.	50.0	2500.0	152.	1.	1.	2.

RESULTS ARE AS FOLLOWS...

THETA	FREQ	REAL	IMAG	PREAL	PIMAG	QREAL	QIMAG
0.01	0.0	1.0000	-0.0010	-0.0000	-0.0011	1.0000	0.0001
0.04	0.1	0.9993	-0.0030	-0.0001	-0.0026	0.9994	-0.0004
0.07	0.3	0.9991	-0.0082	-0.0004	-0.0077	0.9995	-0.0005
0.09	0.5	0.9987	-0.0135	-0.0010	-0.0127	0.9996	-0.0008
0.12	1.0	0.9972	-0.0264	-0.0030	-0.0246	1.0003	-0.0018
0.21	3.0	0.9875	-0.0742	-0.0172	-0.0665	1.0047	-0.0077
0.27	5.0	0.9734	-0.1172	-0.0374	-0.1007	1.0108	-0.0165
0.38	10.0	0.9875	-0.2083	-0.0995	-0.1596	1.0270	-0.0487
0.66	30.0	0.7014	-0.4134	-0.3326	-0.1688	1.0339	-0.2447
0.86	50.0	0.4986	-0.4740	-0.4396	-0.0401	0.9382	-0.4339
1.01	70.0	0.3444	-0.4678	-0.4438	0.0935	0.7882	-0.5614
1.15	90.0	0.2338	-0.4331	-0.3924	0.1918	0.6262	-0.6249
1.27	110.0	0.1567	-0.3887	-0.3195	0.2497	0.4763	-0.6383

NORMALIZING FACTOR = -0.3939E-01

Example 5:



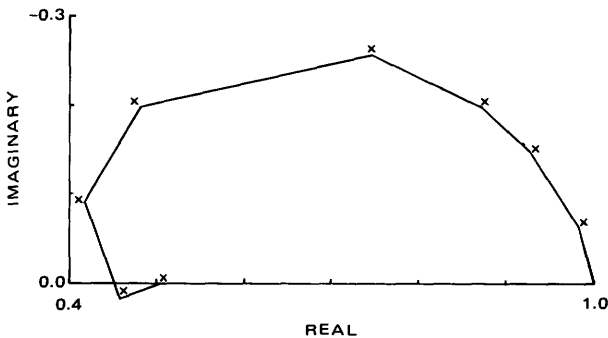
N	A	RHO-1	RHO-2	DEPTH	W	J	M
6.	305.	10.0	0.5	152.	1.	1.	2.

RESULTS ARE AS FOLLOWS...

THETA	FREQ	REAL	IMAG	PREAL	PIMAG	QREAL	QIMAG
0.01	0.0	1.0000	-0.0803	-0.0333	-0.1001	1.0333	0.0198
0.09	0.1	0.6654	-0.1137	-0.4039	-0.3587	1.0692	0.2450
0.15	0.3	0.6051	0.2127	-0.6652	-0.3686	1.2703	0.5814
0.19	0.5	0.7119	0.3803	-0.7379	-0.3996	1.4498	0.7799
0.27	1.0	0.8967	0.5681	-0.8450	-0.5558	1.7417	1.1239
0.47	3.0	1.2442	1.1049	-1.1864	-1.0947	2.4306	2.1996
0.61	5.0	1.5210	1.5459	-1.4582	-1.5277	2.9793	3.0736
0.86	10.0	2.1514	2.4421	-2.0754	-2.4134	4.2268	4.8555
1.48	30.0	4.6624	4.5685	-4.5465	-4.5420	9.2089	9.1105
1.92	50.0	7.0231	5.2227	-6.8955	-5.2197	13.9185	10.4425
2.27	70.0	8.9055	4.9992	-8.7854	-5.0134	17.6908	10.0125
2.57	90.0	10.2276	4.3413	-10.1200	-4.3608	20.3476	8.7021
2.84	110.0	11.0622	3.5410	-10.9635	-3.5582	22.0257	7.0992

NORMALIZING FACTOR = -0.2978E-03

Example 4:



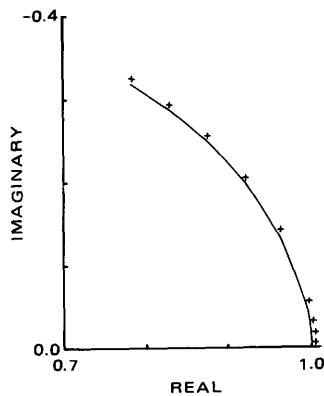
N	A	RHO-1	RHO-2	DEPTH	W	J	M
6.	305.	10.0	10.0	152.	1.	1.	2.

RESULTS ARE AS FOLLOWS...

THETA	FREQ	REAL	IMAG	PREAL	PIMAG	QREAL	QIMAG
0.01	0.0	1.0000	-0.0069	-0.0006	-0.0069	1.0006	-0.0000
0.09	0.1	0.9827	-0.0642	-0.0179	-0.0642	1.0006	-0.0000
0.15	0.3	0.9289	-0.1458	-0.0717	-0.1458	1.0006	0.0000
0.19	0.5	0.8724	-0.1967	-0.1282	-0.1967	1.0006	0.0000
0.27	1.0	0.7458	-0.2553	-0.2547	-0.2553	1.0006	-0.0000
0.47	3.0	0.4797	-0.1980	-0.5209	-0.1980	1.0006	0.0000
0.61	5.0	0.4177	-0.0921	-0.5829	-0.0921	1.0006	-0.0000
0.86	10.0	0.4567	0.0169	-0.5438	0.0169	1.0006	-0.0000
1.48	30.0	0.5066	-0.0006	-0.4940	-0.0006	1.0006	0.0000
1.92	50.0	0.5026	-0.0005	-0.4980	-0.0005	1.0006	0.0000
2.27	70.0	0.5028	0.0000	-0.4977	0.0000	1.0006	0.0000
2.57	90.0	0.5030	-0.0000	-0.4976	-0.0001	1.0006	0.0000
2.84	110.0	0.5029	-0.0001	-0.4976	-0.0001	1.0006	-0.0000

NORMALIZING FACTOR = -0.5949E-02

Example 6:



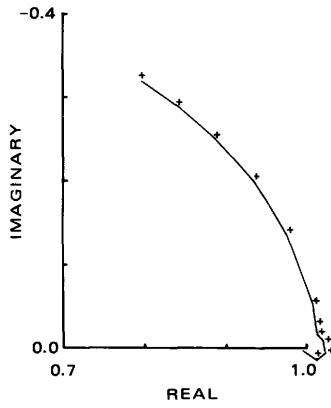
N	A	RHO-1	RHO-2	DEPTH	W	J	M
1.	305.	50.0	1250.0	152.	1.	1.	2.

RESULTS ARE AS FOLLOWS...

THETA	FREQ	REAL	IMAG	PREAL	PIMAG	QREAL	QIMAG
0.01	0.0	1.0000	-0.0001	-0.0000	-0.0003	1.0000	0.0001
0.04	0.1	1.0013	0.0030	-0.0000	-0.0007	1.0013	0.0037
0.07	0.3	1.0069	0.0005	-0.0000	-0.0020	1.0069	0.0025
0.09	0.5	1.0067	-0.0029	-0.0001	-0.0033	1.0068	0.0003
0.12	1.0	1.0050	-0.0063	-0.0003	-0.0065	1.0052	0.0001
0.21	3.0	1.0039	-0.0166	-0.0018	-0.0188	1.0056	0.0021
0.27	5.0	1.0024	-0.0272	-0.0041	-0.0305	1.0065	0.0033
0.38	10.0	0.9972	-0.0521	-0.0123	-0.0574	1.0095	0.0053
0.66	30.0	0.9639	-0.1360	-0.0633	-0.1380	1.0272	0.0020
0.86	50.0	0.9208	-0.2006	-0.1245	-0.1862	1.0453	-0.0144
1.01	70.0	0.8741	-0.2505	-0.1853	-0.2114	1.0595	-0.0391
1.15	90.0	0.8267	-0.2889	-0.2416	-0.2203	1.0683	-0.0686
1.27	110.0	0.7800	-0.3180	-0.2915	-0.2174	1.0715	-0.1006

NORMALIZING FACTOR = -0.5707E+00

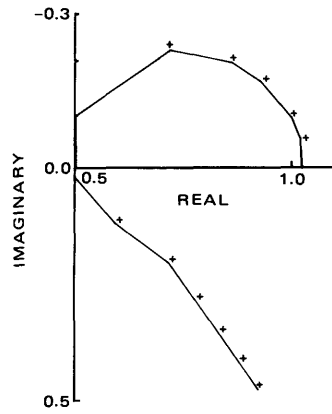
Example 7:



N	A	RHO-1	RHO-2	DEPTH	W	J	M
1.	305.	50.0	2500.0	152.	1.	1.	2.
THETA	FREQ	REAL	IMAG	PREAL	PIMAG	QREAL	QIMAG
0.01	0.0	1.0000	-0.0051	-0.0000	-0.0003	1.0000	-0.0048
0.04	0.1	0.9951	0.0035	-0.0000	-0.0007	0.0051	0.0041
0.07	0.3	1.0125	0.0155	-0.0000	-0.0020	1.0125	0.0175
0.09	0.5	1.0227	0.0070	-0.0001	-0.0033	1.0228	0.0103
0.12	1.0	1.0204	-0.0083	-0.0003	-0.0065	1.0206	-0.0018
0.21	3.0	1.0129	-0.0165	-0.0017	-0.0190	1.0146	0.0025
0.27	5.0	1.0124	-0.0266	-0.0039	-0.0309	1.0164	0.0043
0.38	10.0	1.0075	-0.0514	-0.0121	-0.0584	1.0197	0.0070
0.66	30.0	0.9752	-0.1353	-0.0638	-0.1414	1.0390	0.0061
0.86	50.0	0.9327	-0.2004	-0.1264	-0.1914	1.0590	-0.0089
1.01	70.0	0.8862	-0.2508	-0.1889	-0.2188	1.0751	-0.0329
1.15	90.0	0.8389	-0.2898	-0.2470	-0.2275	1.0858	-0.0622
1.27	110.0	0.7922	-0.3193	-0.2987	-0.2249	1.0909	-0.0944

NORMALIZING FACTOR = -0.5695E+00

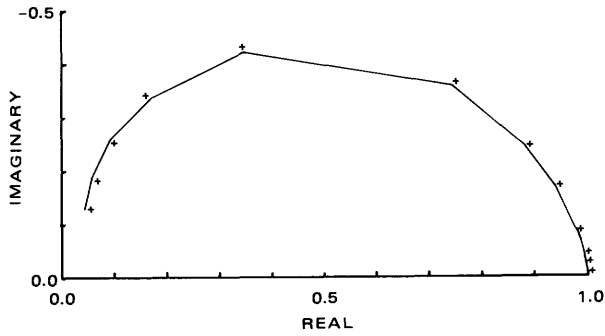
Example 9:



N	A	RHO-1	RHO-2	DEPTH	W	J	M
3.	305.	50.0	2.5	30.	1.	1.	2.
THETA	FREQ	REAL	IMAG	PREAL	PIMAG	QREAL	QIMAG
0.01	0.0	1.0000	-0.0356	-0.0077	-0.0379	1.0077	0.0023
0.04	0.1	0.9838	-0.0720	-0.0238	-0.0775	1.0076	0.0055
0.07	0.3	0.9163	-0.1530	-0.0912	-0.1700	1.0075	0.0171
0.09	0.5	0.8499	-0.1951	-0.1583	-0.2241	1.0082	0.0291
0.12	1.0	0.7143	-0.2223	-0.2990	-0.2811	1.0133	0.0588
0.21	3.0	0.5020	-0.0768	-0.5586	-0.2288	1.0606	0.1520
0.27	5.0	0.45002	0.0498	-0.6143	-0.1585	1.1145	0.2083
0.38	10.0	0.5972	0.1570	-0.6147	-0.1263	1.2119	0.2832
0.66	30.0	0.7116	0.2400	-0.6782	-0.2375	1.3898	0.4775
0.86	50.0	0.7710	0.3224	-0.7391	-0.3149	1.5101	0.6373
1.01	70.0	0.8213	0.3928	-0.7879	-0.3823	1.6092	0.7751
1.15	90.0	0.8651	0.4565	-0.8304	-0.4435	1.6956	0.9000
1.27	110.0	0.9048	0.5156	-0.8689	-0.5005	1.7737	1.0160

NORMALIZING FACTOR = -0.1661E-02

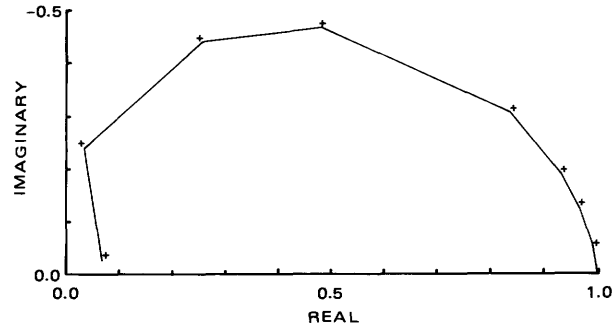
Example 8:



N	A	RHO-1	RHO-2	DEPTH	W	J	M
2.	61.	0.4	3.5	18.0	1.	5.	2.
THETA	FREQ	REAL	IMAG	PREAL	PIMAG	QREAL	QIMAG
0.01	0.0	1.0000	-0.0006	-0.0000	-0.0005	1.0000	-0.0001
0.09	0.1	0.9995	-0.0078	-0.0005	-0.0066	1.0000	-0.0012
0.16	0.3	0.9977	-0.0223	-0.0026	-0.0186	1.0003	-0.0037
0.20	0.5	0.9951	-0.0360	-0.0055	-0.0296	1.0006	-0.0064
0.29	1.0	0.9868	-0.0675	-0.0151	-0.0539	1.0019	-0.0135
0.50	3.0	0.9400	-0.1683	-0.0675	-0.1205	1.0075	-0.0478
0.65	5.0	0.8848	-0.2424	-0.1245	-0.1545	1.0093	-0.0879
0.92	10.0	0.7435	-0.3574	-0.2463	-0.1634	0.9898	-0.1940
1.59	30.0	0.3447	-0.4209	-0.3821	0.0411	0.7268	-0.4620
2.05	50.0	0.1636	-0.3337	-0.3012	0.1599	0.4647	-0.4936
2.42	70.0	0.0859	-0.2462	-0.2084	0.1863	0.2942	-0.4324
2.75	90.0	0.0549	-0.1786	-0.1416	0.1717	0.1965	-0.3503
3.04	110.0	0.0452	-0.1293	-0.1003	0.1436	0.1455	-0.2729

NORMALIZING FACTOR = -0.6572E+00

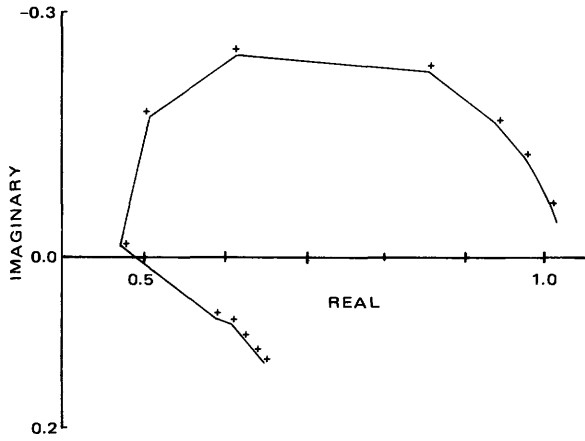
Example 10:



N	A	RHO-1	RHO-2	DEPTH	W	J	M
3.	305.	1.0	10.0	61.	1.	1.	2.
THETA	FREQ	REAL	IMAG	PREAL	PIMAG	QREAL	QIMAG
0.01	0.0	1.0000	-0.0005	-0.0000	-0.0004	1.0000	-0.0001
0.27	0.1	0.9928	-0.0480	-0.0080	-0.0382	1.0008	-0.0098
0.47	0.3	0.9657	-0.1259	-0.0382	-0.0938	1.0040	-0.0322
0.61	0.5	0.9316	-0.1893	-0.0751	-0.1318	1.0068	-0.0575
0.86	1.0	0.8354	-0.3055	-0.1709	-0.1771	1.0063	-0.1284
1.48	3.0	0.4797	-0.4658	-0.4007	-0.0676	0.8804	-0.3982
1.92	5.0	0.2491	-0.4341	-0.4078	0.1060	0.6570	-0.5401
2.71	10.0	0.0342	-0.2386	-0.1828	0.2397	0.2170	-0.4784
4.69	30.0	0.0687	-0.0259	-0.0617	0.0328	0.1304	-0.0587
6.06	50.0	0.0806	-0.0237	-0.0747	0.0249	0.1553	-0.0486
7.17	70.0	0.0757	-0.0192	-0.0713	0.0179	0.1470	-0.0371
8.13	90.0	0.0735	-0.0126	-0.0706	0.0112	0.1441	-0.0238
8.98	110.0	0.0738	-0.0073	-0.0714	0.0065	0.1452	-0.0138

NORMALIZING FACTOR = -0.1987E+00

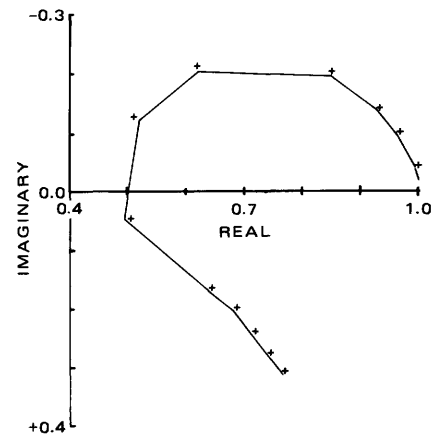
Example 11:



N	H	RHO-1	RHO-2	DEPTH	W	J	M
3	305.	50.0	5.0	15.	1.	1.	2.
RESULTS ARE AS FOLLOWS...							
THETA	FREQ	REAL	IMAG	PREAL	PIMAG	QREAL	QIMAG
0.01	0.0	1.0000	-0.0198	-0.0029	-0.0203	1.0029	0.0005
0.04	0.1	0.9933	-0.0420	-0.0096	-0.0433	1.0029	0.0013
0.07	0.3	0.9625	-0.1013	-0.0403	-0.1053	1.0028	0.0040
0.09	0.5	0.9279	-0.1434	-0.0749	-0.1501	1.0028	0.0068
0.12	1.0	0.8425	-0.2060	-0.1606	-0.2199	1.0031	0.0139
0.21	3.0	0.6057	-0.2261	-0.4046	-0.2673	1.0103	0.0412
0.27	5.0	0.4999	-0.1538	-0.5227	-0.2169	1.0226	0.0631
0.38	10.0	0.4623	-0.0014	-0.5938	-0.0987	1.0561	0.0972
0.66	30.0	0.5776	0.0867	-0.5534	-0.0624	1.1310	0.1491
0.86	50.0	0.5989	0.0946	-0.5707	-0.0938	1.1696	0.1884
1.01	70.0	0.6123	0.1120	-0.5890	-0.1119	1.2014	0.2239
1.15	90.0	0.6260	0.1287	-0.6034	-0.1266	1.2294	0.2554
1.27	110.0	0.6388	0.1435	-0.6158	-0.1403	1.2545	0.2838

NORMALIZING FACTOR = -0.3327E-02

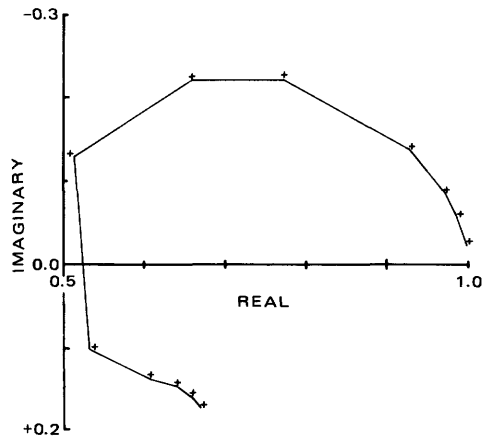
Example 13:



N	A	RHO-1	RHO-2	DEPTH	W	J	M
3	305.	50.0	5.0	30.	1.	1.	2.
RESULTS ARE AS FOLLOWS...							
THETA	FREQ	REAL	IMAG	PREAL	PIMAG	QREAL	QIMAG
0.01	0.0	1.0000	-0.0192	-0.0029	-0.0203	1.0029	0.0011
0.04	0.1	0.9934	-0.0407	-0.0094	-0.0432	1.0029	0.0025
0.07	0.3	0.9630	-0.0976	-0.0397	-0.1054	1.0027	0.0078
0.09	0.5	0.9289	-0.1374	-0.0737	-0.1507	1.0026	0.0132
0.12	1.0	0.8455	-0.1954	-0.1578	-0.2227	1.0033	0.0273
0.21	3.0	0.6171	-0.2026	-0.3997	-0.2837	1.0168	0.0811
0.27	5.0	0.5186	-0.1222	-0.5215	-0.2468	1.0401	0.1246
0.38	10.0	0.4943	0.0436	-0.6099	-0.1512	1.1042	0.1948
0.66	30.0	0.6408	0.1666	-0.6123	-0.1436	1.2531	0.3102
0.86	50.0	0.6834	0.1998	-0.6487	-0.1969	1.3321	0.3968
1.01	70.0	0.7139	0.2389	-0.6832	-0.2361	1.3971	0.4750
1.15	90.0	0.7424	0.2752	-0.7121	-0.2699	1.4545	0.5451
1.27	110.0	0.7687	0.3082	-0.7378	-0.3010	1.5065	0.6093

NORMALIZING FACTOR = -0.3337E-02

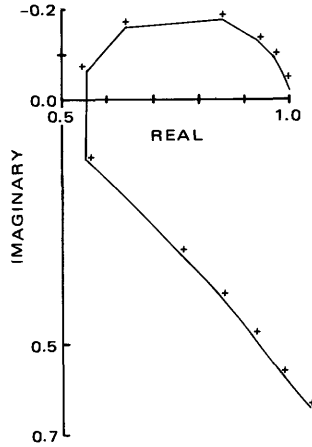
Example 12:



N	A	RHO-1	RHO-2	DEPTH	W	J	M
3	305.	50.0	10.0	30.	1.	1.	2.
RESULTS ARE AS FOLLOWS...							
THETA	FREQ	REAL	IMAG	PREAL	PIMAG	QREAL	QIMAG
0.01	0.0	1.0000	-0.0101	-0.0011	-0.0106	1.0011	0.0005
0.04	0.1	0.9975	-0.0222	-0.0036	-0.0233	1.0011	0.0011
0.07	0.3	0.9847	-0.0575	-0.0163	-0.0608	1.0010	0.0034
0.09	0.5	0.9693	-0.0859	-0.0316	-0.0916	1.0009	0.0057
0.12	1.0	0.9270	-0.1385	-0.0738	-0.1502	1.0008	0.0117
0.21	3.0	0.7696	-0.2220	-0.2335	-0.2585	1.0032	0.0365
0.27	5.0	0.6558	-0.2211	-0.3536	-0.2814	1.0094	0.0603
0.38	10.0	0.5137	-0.1299	-0.5208	-0.2394	1.0345	0.1095
0.66	30.0	0.5340	0.1031	-0.6052	-0.1004	1.1391	0.2035
0.86	50.0	0.6067	0.1387	-0.5957	-0.1073	1.2024	0.2460
1.01	70.0	0.6391	0.1483	-0.6059	-0.1338	1.2451	0.2821
1.15	90.0	0.6570	0.1604	-0.6229	-0.1562	1.2800	0.3166
1.27	110.0	0.6713	0.1752	-0.6401	-0.1742	1.3114	0.3494

NORMALIZING FACTOR = -0.6686E-02

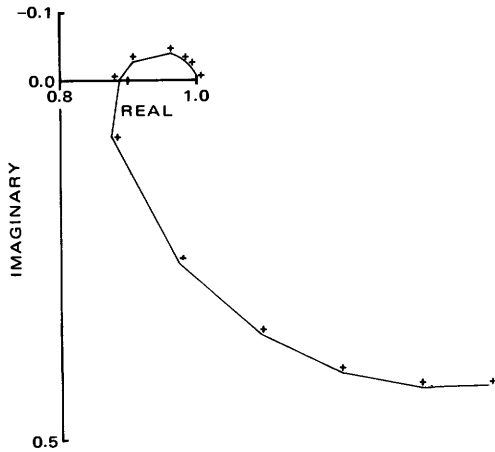
Example 14:



N	A	RHO-1	RHO-2	DEPTH	W	J	M
3	305.	50.0	5.0	61.	1.	1.	2.
RESULTS ARE AS FOLLOWS...							
THETA	FREQ	REAL	IMAG	PREAL	PIMAG	QREAL	QIMAG
0.01	0.0	1.0000	-0.0180	-0.0028	-0.0200	1.0028	0.0020
0.04	0.1	0.9936	-0.0380	-0.0091	-0.0428	1.0027	0.0048
0.07	0.3	0.9642	-0.0900	-0.0382	-0.1048	1.0024	0.0148
0.09	0.5	0.9315	-0.1255	-0.0707	-0.1508	1.0022	0.0253
0.12	1.0	0.8520	-0.1743	-0.1512	-0.2264	1.0032	0.0521
0.21	3.0	0.6399	-0.1575	-0.3870	-0.3131	1.0269	0.1556
0.27	5.0	0.5544	-0.0617	-0.5140	-0.3030	1.0685	0.2413
0.38	10.0	0.5526	0.1325	-0.6326	-0.2545	1.1852	0.3871
0.66	30.0	0.7602	0.3397	-0.7189	-0.3183	1.4791	0.6580
0.86	50.0	0.8500	0.4327	-0.7979	-0.4243	1.6479	0.8571
1.01	70.0	0.9193	0.5226	-0.8690	-0.5128	1.7883	1.0354
1.15	90.0	0.9829	0.6051	-0.9321	-0.5914	1.9150	1.1965
1.27	110.0	1.0424	0.6807	-0.9901	-0.6636	2.0325	1.3443

NORMALIZING FACTOR = -0.3381E-02

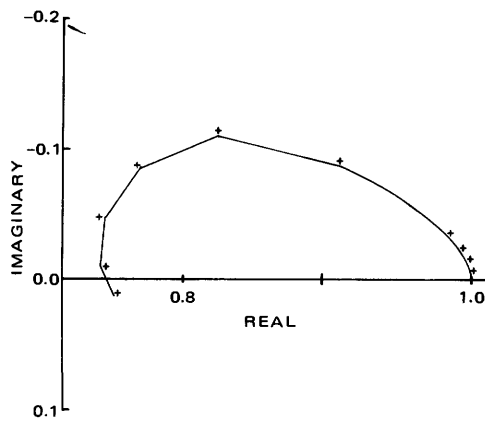
Example 15:



N	A	RHO-1	RHO-2	DEPTH	W	J	M
3	305.	50.0	5.0	305.	1.	1.	2.
THETA	FREQ	REAL	IMAG	PREAL	PIMAG	QREAL	QIMAG
0.01	0.0	1.0000	-0.0046	-0.0008	-0.0063	1.0008	0.0016
0.04	0.1	0.9982	-0.0097	-0.0024	-0.0135	1.0006	0.0038
0.07	0.3	0.9902	-0.0222	-0.0097	-0.0343	1.0000	0.0121
0.09	0.5	0.9816	-0.0303	-0.0177	-0.0512	0.9993	0.0209
0.12	1.0	0.9612	-0.0403	-0.0373	-0.0843	0.9985	0.0440
0.21	3.0	0.9074	-0.0284	-0.1012	-0.1668	1.0086	0.1384
0.27	5.0	0.8834	0.0033	-0.1488	-0.2221	1.0322	0.2254
0.38	10.0	0.8752	0.0803	-0.2385	-0.3273	1.1137	0.4076
0.66	30.0	0.9707	0.2660	-0.5233	-0.6092	1.4941	0.8752
0.86	50.0	1.0884	0.3691	-0.7975	-0.7635	1.8859	1.1327
1.01	70.0	1.2077	0.4280	-1.0546	-0.8240	2.2623	1.2520
1.15	90.0	1.3214	0.4529	-1.2799	-0.8153	2.6013	1.2682
1.27	110.0	1.4243	0.4515	-1.4650	-0.7589	2.8893	1.2104

NORMALIZING FACTOR = -0.1090E-01

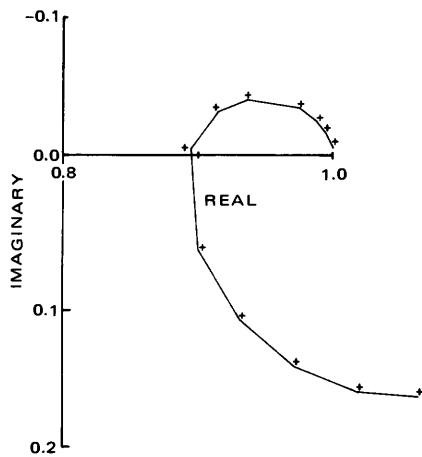
Example 17:



N	A	RHO-1	RHO-2	DEPTH	W	J	M
3.	305	50.0	5.0	457.	1.	1.	2.
THETA	FREQ	REAL	IMAG	PREAL	PIMAG	QREAL	QIMAG
0.01	0.0	1.0000	-0.0028	-0.0004	-0.0032	1.0004	0.0004
0.04	0.1	0.9991	-0.0059	-0.0011	-0.0069	1.0003	0.0009
0.07	0.3	0.9954	-0.0146	-0.0044	-0.0178	0.9997	0.0032
0.09	0.5	0.9913	-0.0211	-0.0079	-0.0270	0.9992	0.0059
0.12	1.0	0.9815	-0.0328	-0.0165	-0.0461	0.9981	0.0133
0.21	3.0	0.9522	-0.0554	-0.0467	-0.1012	0.9990	0.0458
0.27	5.0	0.9328	-0.0665	-0.0727	-0.1436	1.0055	0.0771
0.38	10.0	0.8999	-0.0833	-0.1331	-0.2284	1.0330	0.1451
0.66	30.0	0.8104	-0.1038	-0.3830	-0.4204	1.1934	0.3166
0.86	50.0	0.7531	-0.0798	-0.6168	-0.4558	1.3699	0.3759
1.01	70.0	0.7285	-0.0423	-0.7915	-0.4003	1.5201	0.3580
1.15	90.0	0.7269	-0.0092	-0.8993	-0.3060	1.6262	0.2968
1.27	110.0	0.7373	0.0136	-0.9513	-0.2062	1.6885	0.2198

NORMALIZING FACTOR = -0.2159E-01

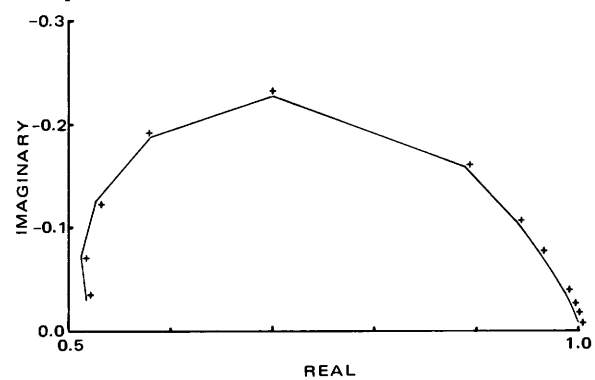
Example 16:



N	A	RHO-1	RHO-2	DEPTH	W	J	M
3	305.	50.0	5.0	366.	1.	1.	2.
THETA	FREQ	REAL	IMAG	PREAL	PIMAG	QREAL	QIMAG
0.01	0.0	1.0000	-0.0035	-0.0005	-0.0044	1.0005	0.0009
0.04	0.1	0.9987	-0.0073	-0.0017	-0.0096	1.0004	0.0023
0.07	0.3	0.9933	-0.0173	-0.0066	-0.0246	0.9998	0.0073
0.09	0.5	0.9873	-0.0242	-0.0119	-0.0369	0.9992	0.0127
0.12	1.0	0.9732	-0.0345	-0.0250	-0.0618	0.9983	0.0273
0.21	3.0	0.9343	-0.0403	-0.0690	-0.1283	1.0033	0.0880
0.27	5.0	0.9138	-0.0313	-0.1037	-0.1761	1.0175	0.1449
0.38	10.0	0.8940	-0.0041	-0.1755	-0.2698	1.0695	0.2657
0.66	30.0	0.8997	0.0685	-0.4358	-0.5061	1.3355	0.5746
0.86	50.0	0.9296	0.1175	-0.6902	-0.6036	1.6197	0.7211
1.01	70.0	0.9705	0.1513	-0.9126	-0.6049	1.8832	0.7562
1.15	90.0	1.0164	0.1692	-1.0863	-0.5454	2.1026	0.7145
1.27	110.0	1.0611	0.1724	-1.2080	-0.4543	2.2691	0.6266

NORMALIZING FACTOR = -0.1538E-01

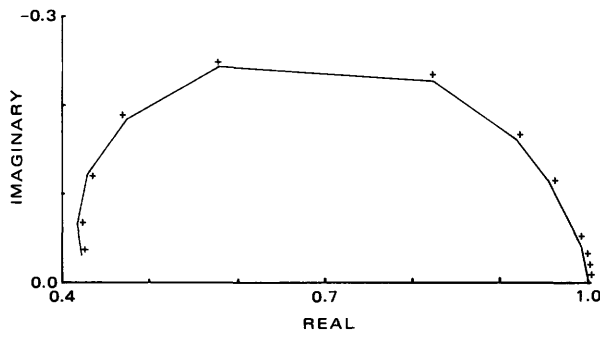
Example 18:



N	A	RHO-1	RHO-2	DEPTH	W	J	M
3	305.	50.0	5.0	610.	1.	1.	2.
THETA	FREQ	REAL	IMAG	PREAL	PIMAG	QREAL	QIMAG
0.01	0.0	1.0000	-0.0025	-0.0003	-0.0024	1.0003	-0.0001
0.04	0.1	0.9994	-0.0054	-0.0008	-0.0053	1.0002	-0.0001
0.07	0.3	0.9967	-0.0138	-0.0030	-0.0138	0.9997	0.0000
0.09	0.5	0.9937	-0.0207	-0.0054	-0.0212	0.9991	0.0005
0.12	1.0	0.9866	-0.0349	-0.0112	-0.0372	0.9978	0.0023
0.21	3.0	0.9618	-0.0740	-0.0334	-0.0871	0.9952	0.0131
0.27	5.0	0.9404	-0.1030	-0.0552	-0.1277	0.9955	0.0247
0.38	10.0	0.8891	-0.1569	-0.1135	-0.2093	1.0026	0.0524
0.66	30.0	0.6984	-0.2272	-0.3741	-0.3528	1.0725	0.1257
0.86	50.0	0.5789	-0.1857	-0.5764	-0.3191	1.1553	0.1334
1.01	70.0	0.5261	-0.1226	-0.6846	-0.2239	1.2107	0.1012
1.15	90.0	0.5123	-0.0690	-0.7220	-0.1281	1.2344	0.0591
1.27	110.0	0.5172	-0.0309	-0.7187	-0.0536	1.2358	0.0227

NORMALIZING FACTOR = -0.3855E-01

Example 19:



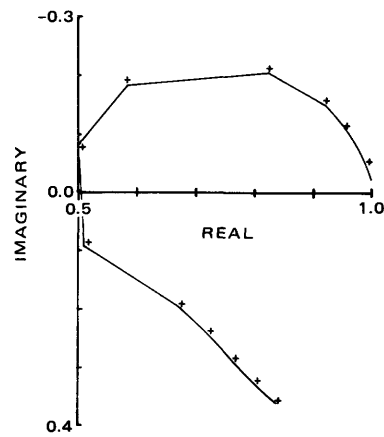
N	A	RHO-1	RHO-2	DEPTH	W	J	M
3	305.	50.0	5.0	1524.	1.	1.	2.

RESULTS ARE AS FOLLOWS...

THETA	FREQ	REAL	IMAG	PREAL	PIMAG	QREAL	QIMAG
0.01	0.0	1.0000	-0.0025	-0.0002	-0.0021	1.0002	-0.0005
0.04	0.1	0.9996	-0.0056	-0.0005	-0.0046	1.0000	-0.0010
0.07	0.3	0.9978	-0.0155	-0.0017	-0.0127	0.9995	-0.0027
0.09	0.5	0.9958	-0.0244	-0.0030	-0.0204	0.9988	-0.0041
0.12	1.0	0.9899	-0.0450	-0.0071	-0.0383	0.9969	-0.0067
0.21	3.0	0.9578	-0.1113	-0.0311	-0.0996	0.9890	-0.0117
0.27	5.0	0.9188	-0.1592	-0.0635	-0.1476	0.9824	-0.0116
0.38	10.0	0.8214	-0.2261	-0.1541	-0.2211	0.9755	-0.0050
0.66	30.0	0.5771	-0.2425	-0.4042	-0.2443	0.9812	0.0018
0.86	50.0	0.4707	-0.1801	-0.5108	-0.1799	0.9815	-0.0002
1.01	70.0	0.4277	-0.1161	-0.5531	-0.1158	0.9808	-0.0003
1.15	90.0	0.4175	-0.0651	-0.5632	-0.0651	0.9807	-0.0000
1.27	110.0	0.4229	-0.0290	-0.5578	-0.0290	0.9808	0.0000

NORMALIZING FACTOR = -0.3398E-01

Example 21:



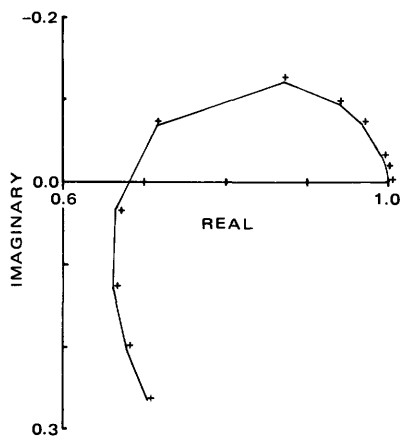
N	A	RHO-1	RHO-2	DEPTH	W	J	M
5.	305.	50.0	10.0	61.	1.	1.	2.

RESULTS ARE AS FOLLOWS...

THETA	FREQ	REAL	IMAG	PREAL	PIMAG	QREAL	QIMAG
0.01	0.0	1.0000	-0.0218	-0.0036	-0.0232	1.0036	0.0014
0.04	0.1	0.9921	-0.0459	-0.0114	-0.0492	1.0035	0.0034
0.07	0.3	0.9560	-0.1079	-0.0473	-0.1183	1.0033	0.0104
0.09	0.5	0.9164	-0.1495	-0.0869	-0.1672	1.0033	0.0177
0.12	1.0	0.8220	-0.2049	-0.1825	-0.2414	1.0045	0.0365
0.21	3.0	0.5845	-0.1825	-0.4408	-0.2889	1.0252	0.1064
0.27	5.0	0.5005	-0.0821	-0.5581	-0.2423	1.0586	0.1602
0.38	10.0	0.5136	0.0893	-0.6297	-0.1514	1.1433	0.2407
0.66	30.0	0.6739	0.1915	-0.6484	-0.1815	1.3223	0.3730
0.86	50.0	0.7225	0.2367	-0.7018	-0.2404	1.4244	0.4771
1.01	70.0	0.7645	0.2824	-0.7469	-0.2838	1.5114	0.5662
1.15	90.0	0.8034	0.3219	-0.7856	-0.3216	1.5890	0.6435
1.27	110.0	0.8390	0.3568	-0.8209	-0.3556	1.6599	0.7124

NORMALIZING FACTOR = -0.1911E-02

Example 20:



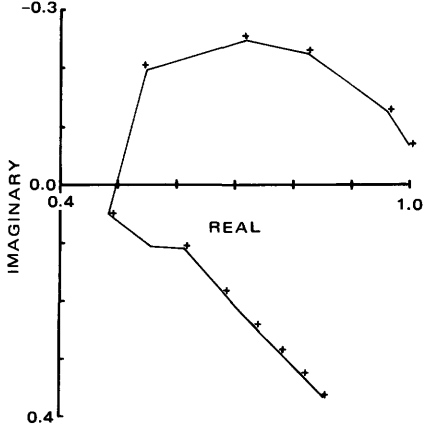
N	A	RHO-1	RHO-2	DEPTH	W	J	M
1	305.	50.0	10.0	61.	1.	1.	2.

RESULTS ARE AS FOLLOWS...

THETA	FREQ	REAL	IMAG	PREAL	PIMAG	QREAL	QIMAG
0.01	0.0	1.0000	-0.0017	-0.0001	-0.0020	1.0001	0.0003
0.04	0.1	0.9998	-0.0039	-0.0003	-0.0046	1.0001	0.0007
0.07	0.3	0.9984	-0.0109	-0.0016	-0.0130	1.0001	0.0021
0.09	0.5	0.9967	-0.0172	-0.0033	-0.0207	1.0000	0.0036
0.12	1.0	0.9914	-0.0310	-0.0085	-0.0383	0.9999	0.0073
0.21	3.0	0.9649	-0.0700	-0.0344	-0.0929	0.9993	0.0226
0.27	5.0	0.9366	-0.0947	-0.0635	-0.1332	0.9990	0.0385
0.38	10.0	0.8711	-0.1214	-0.1297	-0.2009	1.0008	0.0795
0.66	30.0	0.7155	-0.0665	-0.3212	-0.3016	1.0368	0.2352
0.86	50.0	0.6654	0.0353	-0.4310	-0.3293	1.0964	0.3645
1.01	70.0	0.6622	0.1270	-0.5011	-0.3435	1.1633	0.4705
1.15	90.0	0.6801	0.2030	-0.5508	-0.3560	1.2309	0.5590
1.27	110.0	0.7072	0.2653	-0.5894	-0.3693	1.2966	0.6346

NORMALIZING FACTOR = -0.7602E-01

Example 22:



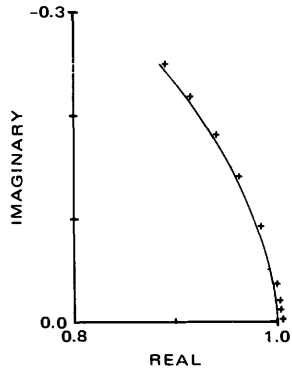
N	A	RHO-1	RHO-2	DEPTH	W	J	M
10.	305.	50.0	10.0	61	1.	1.	2.

RESULTS ARE AS FOLLOWS...

THETA	FREQ	REAL	IMAG	PREAL	PIMAG	QREAL	QIMAG
0.01	0.0	1.0000	-0.0664	-0.0195	-0.0692	1.0195	0.0028
0.04	0.1	0.9620	-0.1256	-0.0574	-0.1323	1.0194	0.0068
0.07	0.3	0.8258	-0.2245	-0.1944	-0.2457	1.0202	0.0212
0.09	0.5	0.7150	-0.2471	-0.3081	-0.2827	1.0231	0.0356
0.12	1.0	0.5467	-0.1963	-0.4893	-0.2636	1.0360	0.0672
0.21	3.0	0.4826	0.0461	-0.6202	-0.0884	1.1028	0.1346
0.27	5.0	0.5548	0.1007	-0.5936	-0.0612	1.1484	0.1619
0.38	10.0	0.6134	0.1075	-0.5962	-0.1047	1.2096	0.2122
0.66	30.0	0.6822	0.1838	-0.6767	-0.1850	1.3589	0.3688
0.86	50.0	0.7354	0.2395	-0.7299	-0.2404	1.4653	0.4799
1.01	70.0	0.7797	0.2854	-0.7742	-0.2859	1.5539	0.5713
1.15	90.0	0.8188	0.3251	-0.8134	-0.3254	1.6322	0.6505
1.27	110.0	0.8546	0.3607	-0.8492	-0.3607	1.7038	0.7214

NORMALIZING FACTOR = -0.2978E-03

Example 23:



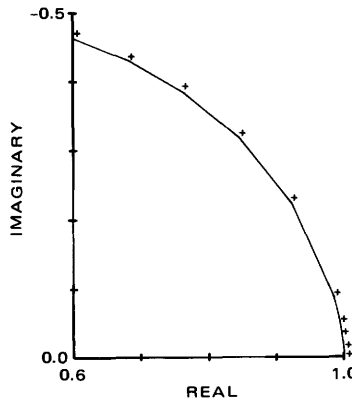
N	A	RHO-1	RHO-2	DEPTH	W	J	M
1.	305.	50.0	500.0	61.	1.	1.	2.

RESULTS ARE AS FOLLOWS...

THETA	FREQ	REAL	IMAG	PREAL	PIMAG	QREAL	QIMAG
0.01	0.0	1.0000	-0.0001	-0.0000	-0.0001	1.0000	0.0001
0.04	0.1	1.0001	-0.0003	-0.0000	-0.0003	1.0001	0.0001
0.07	0.3	1.0001	-0.0011	-0.0000	-0.0010	1.0001	-0.0001
0.09	0.5	1.0001	-0.0018	-0.0000	-0.0016	1.0001	-0.0002
0.12	1.0	1.0000	-0.0035	-0.0001	-0.0031	1.0001	-0.0004
0.21	3.0	0.9995	-0.0103	-0.0007	-0.0091	1.0002	-0.0013
0.27	5.0	0.9987	-0.0169	-0.0016	-0.0148	1.0003	-0.0021
0.38	10.0	0.9962	-0.0326	-0.0046	-0.0282	1.0009	-0.0044
0.66	30.0	0.9808	-0.0884	-0.0236	-0.0729	1.0044	-0.0155
0.86	50.0	0.9603	-0.1362	-0.0484	-0.1070	1.0086	-0.0292
1.01	70.0	0.9370	-0.1778	-0.0757	-0.1327	1.0127	-0.0450
1.15	90.0	0.9120	-0.2142	-0.1039	-0.1518	1.0159	-0.0624
1.27	110.0	0.8859	-0.2462	-0.1322	-0.1651	1.0181	-0.0811

NORMALIZING FACTOR = -0.1169E+01

Example 25:



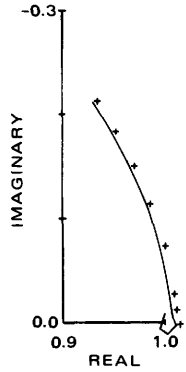
N	A	RHO-1	RHO-2	DEPTH	W	J	M
5	305.	50.0	5000.0	61.	1.	1.	2.

RESULTS ARE AS FOLLOWS...

THETA	FREQ	REAL	IMAG	PREAL	PIMAG	QREAL	QIMAG
0.01	0.0	1.0000	0.0000	-0.0000	-0.0000	1.0000	0.0001
0.04	0.1	1.0012	-0.0006	-0.0000	-0.0009	1.0012	0.0003
0.07	0.3	1.0005	-0.0031	-0.0001	-0.0027	1.0006	-0.0004
0.09	0.5	1.0003	-0.0048	-0.0002	-0.0045	1.0005	-0.0004
0.12	1.0	1.0001	-0.0096	-0.0005	-0.0088	1.0007	-0.0009
0.21	3.0	0.9982	-0.0260	-0.0032	-0.0252	1.0014	-0.0028
0.27	5.0	0.9953	-0.0456	-0.0073	-0.0405	1.0027	-0.0050
0.38	10.0	0.9853	-0.0866	-0.0217	-0.0743	1.0070	-0.0123
0.66	30.0	0.9228	-0.2199	-0.1055	-0.1598	1.0283	-0.0601
0.86	50.0	0.8643	-0.3158	-0.1969	-0.1886	1.0412	-0.1272
1.01	70.0	0.7618	-0.3836	-0.2777	-0.1807	1.0395	-0.2029
1.15	90.0	0.6808	-0.4300	-0.3420	-0.1501	1.0229	-0.2799
1.27	110.0	0.6042	-0.4600	-0.3889	-0.1065	0.9931	-0.3535

NORMALIZING FACTOR = -0.1337E+00

Example 24:



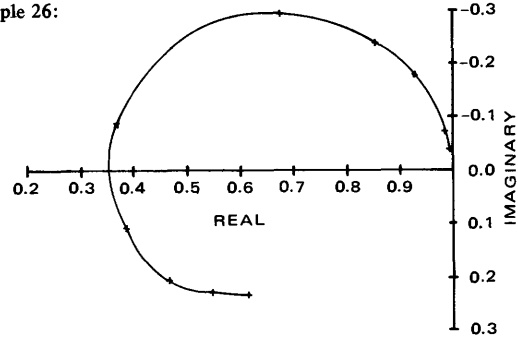
N	A	RHO-1	RHO-2	DEPTH	W	J	M
1.	305.	50.0	5000.0	61.	1.	1.	2.

RESULTS ARE AS FOLLOWS...

THETA	FREQ	REAL	IMAG	PREAL	PIMAG	QREAL	QIMAG
0.01	0.0	1.0000	-0.0040	-0.0000	-0.0001	1.0000	-0.0039
0.04	0.1	0.9960	-0.0030	-0.0000	-0.0003	0.9960	-0.0028
0.07	0.3	0.9949	0.0063	-0.0000	-0.0008	0.9949	0.0071
0.09	0.5	1.0013	0.0100	-0.0000	-0.0013	1.0013	0.0114
0.12	1.0	1.0114	0.0046	-0.0001	-0.0026	1.0114	0.0072
0.21	3.0	1.0075	-0.0100	-0.0004	-0.0078	1.0079	-0.0021
0.27	5.0	1.0054	-0.0134	-0.0009	-0.0129	1.0063	-0.0005
0.38	10.0	1.0048	-0.0246	-0.0029	-0.0250	1.0077	0.0005
0.66	30.0	0.9959	-0.0699	-0.0173	-0.0692	1.0132	-0.0017
0.86	50.0	0.9826	-0.1107	-0.0380	-0.1035	1.0206	-0.0072
1.01	70.0	0.9664	-0.1477	-0.0621	-0.1320	1.0286	-0.0156
1.15	90.0	0.9483	-0.1812	-0.0882	-0.1546	1.0365	-0.0265
1.27	110.0	0.9287	-0.2115	-0.1151	-0.1720	1.0438	-0.0395

NORMALIZING FACTOR = -0.1417E+01

Example 26:



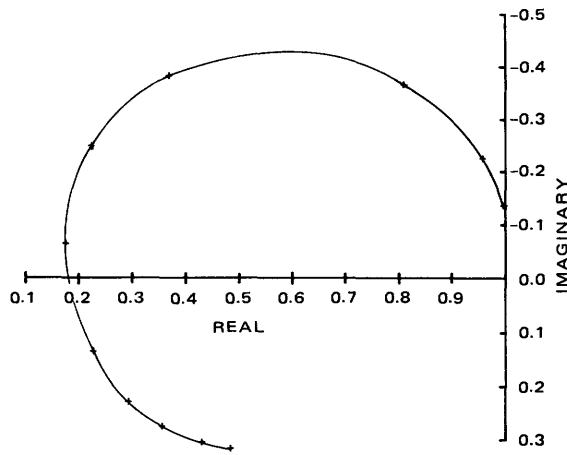
N	A	RHO-1	RHO-2	DEPTH	W	J	M	RHO-3
3.	305.	50.0	10.0	61.	1.	1.	2.	50.0

RESULTS ARE AS FOLLOWS...

THETA	FREQ	REAL	IMAG	PREAL	PIMAG	QREAL	QIMAG
0.025	0.0	1.0000	-0.0033	-0.0004	-0.0035	1.0004	0.0001
0.038	0.1	0.9998	-0.0078	-0.0012	-0.0076	1.0010	-0.0001
0.066	0.3	0.9983	-0.0228	-0.0052	-0.0200	1.0035	-0.0028
0.086	0.5	0.9958	-0.0372	-0.0101	-0.0301	1.0059	-0.0070
0.121	1.0	0.9866	-0.0707	-0.0236	-0.0498	1.0102	-0.0210
0.210	3.0	0.9263	-0.1746	-0.0746	-0.0883	1.0008	-0.0863
0.271	5.0	0.8518	-0.2397	-0.1135	-0.0997	0.9653	-0.1400
0.383	10.0	0.6736	-0.2969	-0.1707	-0.0956	0.8443	-0.2013
0.664	30.0	0.3645	-0.0880	-0.2172	-0.0694	0.5817	-0.0186
0.857	50.0	0.3819	0.1077	-0.2264	-0.0789	0.6084	0.1866
1.014	70.0	0.4664	0.2023	-0.2378	-0.0933	0.7042	0.2956
1.149	90.0	0.5485	0.2376	-0.2500	-0.1064	0.7985	0.3440
1.271	110.0	0.6143	0.2433	-0.2616	-0.1177	0.8760	0.3610

NORMALIZING FACTOR = -0.2043E-01

Example 27:



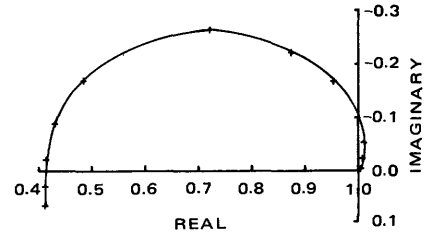
N	A	RHO-1	RHO-2	DEPTH	W	J	M	RHO-3
3.	305.	50.0	1.0	61.	1.	1.	2.	50.0

RESULTS ARE AS FOLLOWS...

THETA	FREQ	REAL	IMAG	PREAL	PIMAG	QREAL	QIMAG
0.025	0.0	1.0000	-0.0110	-0.0010	-0.0031	1.0010	-0.0079
0.038	0.1	1.0062	-0.0356	-0.0027	-0.0058	1.0089	-0.0298
0.066	0.3	0.9969	-0.1356	-0.0085	-0.0104	1.0055	-0.1252
0.086	0.5	0.9563	-0.2244	-0.0130	-0.0120	0.9693	-0.2125
0.121	1.0	0.8079	-0.3657	-0.0197	-0.0121	0.8275	-0.3537
0.210	3.0	0.3676	-0.3810	-0.0257	-0.0106	0.3933	-0.3704
0.271	5.0	0.2205	-0.2495	-0.0272	-0.0128	0.2477	-0.2367
0.383	10.0	0.1641	-0.0672	-0.0311	-0.0192	0.1952	-0.0480
0.664	30.0	0.2152	0.1431	-0.0420	-0.0386	0.2572	0.1817
0.857	50.0	0.2922	0.2317	-0.0499	-0.0549	0.3420	0.2866
1.014	70.0	0.3654	0.2792	-0.0567	-0.0697	0.4221	0.3489
1.149	90.0	0.4295	0.3044	-0.0630	-0.0836	0.4925	0.3880
1.127	110.0	0.4839	0.3168	-0.0689	-0.0968	0.5529	0.4136

NORMALIZING FACTOR = -0.1763E-01

Example 29:



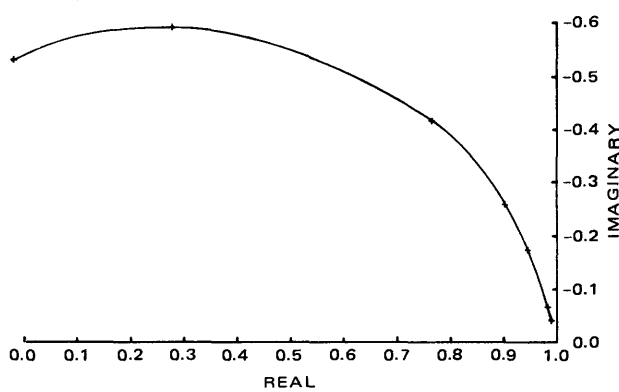
N	A	RHO-1	RHO-2	DEPTH	W	J	M	RHO-3
1.	305.	50.0	1.0	61.	1.	1.	2.	50.0

RESULTS ARE AS FOLLOWS...

THETA	FREQ	REAL	IMAG	PREAL	PIMAG	QREAL	QIMAG
0.025	0.0	1.0000	-0.0001	-0.0001	-0.0007	1.0001	0.0006
0.038	0.1	1.0015	-0.0016	-0.0003	-0.0015	1.0018	-0.0001
0.066	0.3	1.0061	-0.0107	-0.0013	-0.0036	1.0074	-0.0071
0.086	0.5	1.0090	-0.0228	-0.0023	-0.0052	1.0114	-0.0176
0.121	1.0	1.0089	-0.0563	-0.0049	-0.0079	1.0137	-0.0484
0.210	3.0	0.9545	-0.1661	-0.0120	-0.0126	0.9665	-0.1534
0.271	5.0	0.8789	-0.2261	-0.0161	-0.0146	0.8950	-0.2115
0.383	10.0	0.7227	-0.2664	-0.0215	-0.0181	0.7443	-0.2483
0.664	30.0	0.4896	-0.1694	-0.0307	-0.0318	0.5203	-0.1376
0.857	50.0	0.4336	-0.0854	-0.0370	-0.0447	0.4706	-0.0408
1.014	70.0	0.4160	-0.0252	-0.0424	-0.0565	0.4584	0.0314
1.149	90.0	0.4129	0.0221	-0.0474	-0.0678	0.4603	0.0898
1.127	110.0	0.4171	0.0611	-0.0521	-0.0785	0.4692	0.1396

NORMALIZING FACTOR = -0.1971E+00

Example 28:



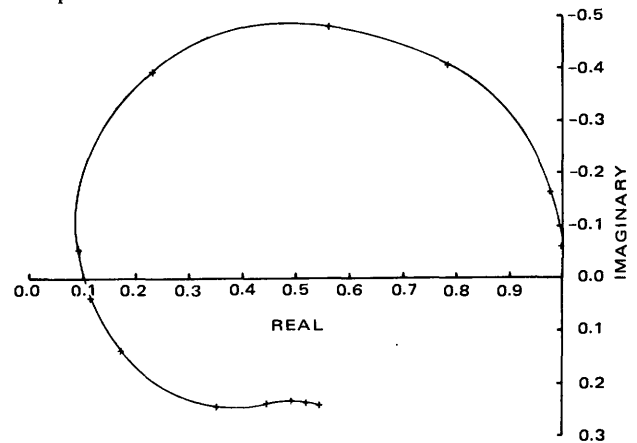
N	A	RHO-1	RHO-2	DEPTH	W	J	M	RHO-3
3.	305.	50.0	50.0	61.	1.	1.	2.	1.0

RESULTS ARE AS FOLLOWS...

THETA	FREQ	REAL	IMAG	PREAL	PIMAG	QREAL	QIMAG
0.025	0.0	1.0000	-0.0040	-0.0002	-0.0044	1.0002	0.0005
0.038	0.1	0.9992	-0.0086	-0.0007	-0.0101	0.9999	0.0015
0.066	0.3	0.9963	-0.0230	-0.0035	-0.0286	0.9998	0.0056
0.086	0.5	0.9935	-0.0359	-0.0072	-0.0458	1.0007	0.0098
0.121	1.0	0.9865	-0.0660	-0.0189	-0.0846	1.0054	0.0186
0.210	3.0	0.9499	-0.1725	-0.0800	-0.2053	1.0299	0.0328
0.271	5.0	0.9007	-0.2597	-0.1487	-0.2917	1.0495	0.0320
0.383	10.0	0.7610	-0.4120	-0.3190	-0.4236	1.0800	0.0116
0.664	30.0	0.2774	-0.5898	-0.7988	-0.4888	1.0762	-0.1010
0.857	50.0	-0.0256	-0.5257	-1.0210	-0.3635	0.9954	-0.1622
1.014	70.0	-0.2021	-0.4022	-1.1072	-0.2323	0.9052	-0.1699
1.149	90.0	-0.2990	-0.2723	-1.1266	-0.1297	0.8277	-0.1427
1.127	110.0	-0.3463	-0.1531	-1.1152	-0.0576	0.7689	-0.0955

NORMALIZING FACTOR = -0.1700E-01

Example 30:



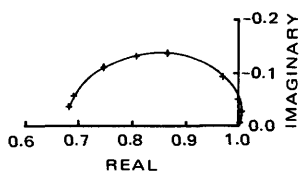
N	A	RHO-1	RHO-2	DEPTH	W	J	M	RHO-3
6.	305.	50.0	1.0	61.	1.	1.	2.	50.0

RESULTS ARE AS FOLLOWS...

THETA	FREQ	REAL	IMAG	PREAL	PIMAG	QREAL	QIMAG
0.025	0.0	1.0000	-0.0616	-0.0040	-0.0071	1.0040	-0.0545
0.038	0.1	0.9840	-0.1653	-0.0094	-0.0104	0.9934	-0.1549
0.066	0.3	0.7841	-0.4082	-0.0199	-0.0104	0.8040	-0.3978
0.086	0.5	0.5653	-0.4812	-0.0233	-0.0079	0.5886	-0.4733
0.121	1.0	0.2360	-0.3939	-0.0243	-0.0056	0.2603	-0.3883
0.210	3.0	0.0906	-0.0567	-0.0262	-0.0096	0.1168	-0.0470
0.271	5.0	0.1127	0.0323	-0.0286	-0.0129	0.1413	0.0452
0.383	10.0	0.1686	0.1335	-0.0330	-0.0195	0.2015	0.1530
0.664	30.0	0.3517	0.2317	-0.0441	-0.0396	0.3958	0.2713
0.857	50.0	0.4446	0.2320	-0.0522	-0.0564	0.4968	0.2884
1.014	70.0	0.4930	0.2265	-0.0592	-0.0717	0.5522	0.2982
1.149	90.0	0.5237	0.2269	-0.0657	-0.0860	0.5894	0.3129
1.127	110.0	0.5480	0.2319	-0.0719	-0.0997	0.6199	0.3315

NORMALIZING FACTOR = -0.3109E-02

Example 31:



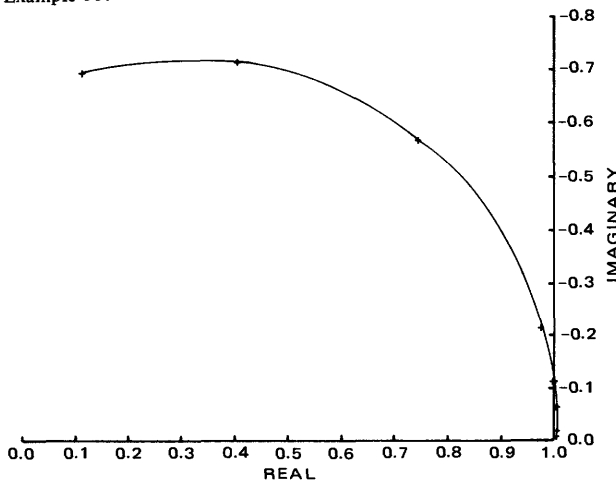
N	A	RHO-1	RHO-2	DEPTH	W	J	M	RHO-3
3.	305.	50.0	1.0	305.	1.	1.	2.	50.0

RESULTS ARE AS FOLLOWS...

THETA	FREQ	REAL	IMAG	PREAL	PIMAG	QREAL	QIMAG
0.025	0.0	1.0000	0.0004	-0.0005	-0.0022	1.0005	0.0026
0.038	0.1	1.0039	-0.0043	-0.0015	-0.0044	1.0053	0.0001
0.066	0.3	1.0066	-0.0288	-0.0045	-0.0096	1.0111	-0.0192
0.086	0.5	0.9997	-0.0518	-0.0070	-0.0133	1.0067	-0.0385
0.121	1.0	0.9696	-0.0918	-0.0116	-0.0204	0.9811	-0.0714
0.210	3.0	0.8652	-0.1332	-0.0223	-0.0421	0.8875	-0.0912
0.271	5.0	0.8096	-0.1295	-0.0299	-0.0612	0.8395	-0.0683
0.383	10.0	0.7460	-0.1073	-0.0474	-0.1047	0.7934	-0.0026
0.664	30.0	0.6886	-0.0544	-0.1296	-0.2453	0.8182	0.1909
0.857	50.0	0.6855	-0.0384	-0.2342	-0.3431	0.9197	0.3046
1.014	70.0	0.6848	-0.0397	-0.3491	-0.4003	1.0338	0.3606
1.149	90.0	0.6782	-0.0454	-0.4620	-0.4212	1.1402	0.3759
1.271	110.0	0.6671	-0.0488	-0.5639	-0.4127	1.2311	0.3639

NORMALIZING FACTOR = -0.2566E-01

Example 33:



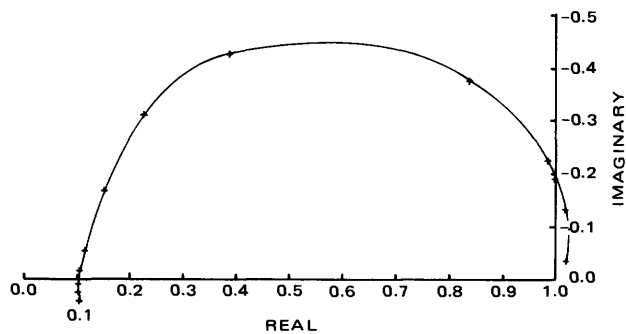
N	A	RHO-1	RHO-2	DEPTH	W	J	M	RHO-3
3.	305.	10.0	1000.0	61.	1.	1.	2.	50.0

RESULTS ARE AS FOLLOWS...

THETA	FREQ	REAL	IMAG	PREAL	PIMAG	QREAL	QIMAG
0.025	0.0	1.0000	0.0006	-0.0000	-0.0001	1.0000	0.0007
0.086	0.1	1.0057	-0.0024	-0.0000	-0.0007	1.0057	-0.0017
0.148	0.3	1.0050	-0.0067	-0.0001	-0.0020	1.0051	-0.0046
0.192	0.5	1.0049	-0.0111	-0.0003	-0.0033	1.0052	-0.0077
0.271	1.0	1.0046	-0.0221	-0.0008	-0.0065	1.0055	-0.0156
0.469	3.0	1.0023	-0.0660	-0.0048	-0.0174	1.0072	-0.0486
0.606	5.0	0.9977	-0.1101	-0.0105	-0.0262	1.0081	-0.0840
0.857	10.0	0.9740	-0.2191	-0.0276	-0.0403	1.0017	-0.1788
1.484	30.0	0.7378	-0.5667	-0.0867	-0.0349	0.8245	-0.5319
1.916	50.0	0.4094	-0.7128	-0.1070	0.0024	0.5164	-0.7153
2.267	70.0	0.1165	-0.6958	-0.1007	0.0355	0.2172	-0.7313
2.570	90.0	-0.0928	-0.5879	-0.0828	0.0562	-0.0100	-0.6440
2.841	110.0	-0.2170	-0.4466	-0.0625	0.0657	-0.1544	-0.5123

NORMALIZING FACTOR = -0.1314E+01

Example 32:



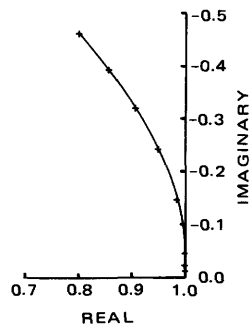
N	A	RHO-1	RHO-2	DEPTH	W	J	M	RHO-3
3.	305.	500.0	1.0	61.	1.	1.	2.	500.0

RESULTS ARE AS FOLLOWS...

THETA	FREQ	REAL	IMAG	PREAL	PIMAG	QREAL	QIMAG
0.025	0.4	1.0000	-0.1934	-0.0012	-0.0012	1.0012	-0.1922
0.012	0.1	1.0244	-0.0318	-0.0003	-0.0006	1.0246	-0.0312
0.021	0.3	1.0210	-0.1323	-0.0009	-0.0011	1.0219	-0.1313
0.027	0.5	0.9841	-0.2247	-0.0013	-0.0012	0.9854	-0.2234
0.038	1.0	0.8386	-0.3769	-0.0020	-0.0013	0.8406	-0.3757
0.066	3.0	0.3875	-0.4225	-0.0027	-0.0011	0.3902	-0.4214
0.086	5.0	0.2292	-0.3092	-0.0028	-0.0014	0.2320	-0.3079
0.124	10.0	0.1509	-0.1632	-0.0032	-0.0021	0.1542	-0.1612
0.210	30.0	0.1158	-0.0537	-0.0043	-0.0042	0.1201	-0.0496
0.271	50.0	0.1073	-0.0182	-0.0051	-0.0060	0.1123	-0.0122
0.321	70.0	0.1043	0.0052	-0.0057	-0.0077	0.1100	0.0129
0.363	90.0	0.1037	0.0240	-0.0062	-0.0093	0.1099	0.0333
0.402	110.0	0.1046	0.0404	-0.0067	-0.0109	0.1113	0.0512

NORMALIZING FACTOR = -0.1708E-01

Example 34:



N	A	RHO-1	RHO-2	DEPTH	W	J	M	RHO-3
3.	305.	10.0	10000.0	9.	1.	5.	2.	200.0

RESULTS ARE AS FOLLOWS...

THETA	FREQ	REAL	IMAG	PREAL	PIMAG	QREAL	QIMAG
0.025	0.0	1.0000	-0.0006	-0.0000	-0.0000	1.0000	-0.0006
0.086	0.1	1.0001	0.0021	-0.0000	-0.0001	1.0001	0.0022
0.148	0.3	1.0038	0.0005	-0.0000	-0.0003	1.0038	0.0008
0.192	0.5	1.0041	-0.0020	-0.0000	-0.0005	1.0041	-0.0015
0.271	1.0	1.0033	-0.0051	-0.0000	-0.0010	1.0034	-0.0042
0.469	3.0	1.0030	-0.0149	-0.0003	-0.0028	1.0033	-0.0120
0.606	5.0	1.0028	-0.0248	-0.0006	-0.0046	1.0034	-0.0202
0.857	10.0	1.0015	-0.0497	-0.0019	-0.0087	1.0034	-0.0410
1.484	30.0	0.9859	-0.1487	-0.0101	-0.0209	0.9960	-0.1278
1.916	50.0	0.9547	-0.2413	-0.0202	-0.0278	0.9748	-0.2135
2.267	70.0	0.9117	-0.3248	-0.0303	-0.0308	0.9419	-0.2939
2.570	90.0	0.8601	-0.3980	-0.0396	-0.0310	0.8997	-0.3670
2.841	110.0	0.8026	-0.4608	-0.0477	-0.0291	0.8503	-0.4317

NORMALIZING FACTOR = -0.3237E+02

SELECTED REFERENCES

- Abramowitz, Milton, and Stegun, I. A., 1964, Handbook of mathematical functions — with formulas, graphs, and mathematical tables: National Bureau of Standards Applied Mathematics Series 55, 1046 p.
- Anderson, W. L., 1975, Improved digital filters for evaluating Fourier and Hankel transform integrals: Available only from National Technical Information Service, Springfield, Va. 22161, as NTIS PB-242 800, 119 p.
- Dey, Abhijit, and Morrison, H. F., 1973, Electromagnetic coupling in frequency and time-domain induced-polarization surveys over a multilayered earth: *Geophysics*, v. 38, no. 2, p. 380-405.
- Hallof, P. G., 1974, The IP phase measurement and inductive coupling: *Geophysics*, v. 39, no. 5, p. 650-665.
- Hohmann, G. W., 1973, Electromagnetic coupling between grounded wires at the surface of a two-layer earth: *Geophysics*, v. 38, no. 5, p. 854-863.
- 1975, Three-dimensional induced polarization and electromagnetic coupling: *Geophysics*, v. 40, no. 2, p. 309-324.
- Jahnke, Eugene, and Emde, Fritz, 1945, Tables of functions: New York, Dover, 380 p.
- Millett, F. B., Jr., 1967, Electromagnetic coupling of collinear dipoles on a uniform half-space, in *Mining Geophysics, Volume II, Theory: Soc. Exploration Geophysicists*, p. 401-419.
- Riordan, J., and Sunde, E. D., 1933, Mutual impedance of grounded wires for stratified two-layer earth: *Bell Syst. Tech. Jour.*, v. 12, p. 162.
- Sumner, J. S., 1976, Principles of induced polarization for geophysical exploration: New York, Elsevier, *Developments in economic geology*, 5, 277 p.
- Sunde, E. D., 1968, Earth conduction effects in transmission systems: New York, Dover, 370 p.
- Wait, J. R., 1966, Fields of a horizontal dipole over a stratified anisotropic half-space: *IEEE Trans. on Antennas and Propagation*, v. AP-14, no. 6, p. 790-792.
- Wynn, J. C., 1974, Electromagnetic coupling in induced polarization: Arizona University Ph.D. thesis, 137 p.
- Wynn, J. C., and Zonge, K. L., 1975, EM coupling, its intrinsic value, its removal and the cultural coupling problem: *Geophysics*, v. 40, no. 5, p. 831-850.
- Zonge, K. L., and Wynn, J. C., 1975, Recent advances and applications in complex resistivity measurements: *Geophysics*, v. 40, no. 5, p. 851-864.
- Zonge, K. L., Wynn, J. C., and Young, G. N., 1976, Complex resistivity case histories [abs.]: *Geophysics*, v. 41, no. 2, p. 382-383.